

# CHALMERS



## Development of an ASPEN Plus model of a Chemical-looping reformer reactor

*Master of Science Thesis*

DANIEL CHRISTOPH FERNANDES LOHSE

Department of Energy and Environment  
*Division of Energy Technology*  
CHALMERS UNIVERSITY OF TECHNOLOGY  
Göteborg, Sweden, 2011  
Master's Thesis 2011: T2011-362



MASTER'S THESIS 2011:T2011-362

# Development of an ASPEN Plus model of a Chemical-looping reformer reactor

Master's Thesis

DANIEL CHRISTOPH FERNANDES LOHSE

Department of Energy and Environment  
*Division of Energy Technology*  
CHALMERS UNIVERSITY OF TECHNOLOGY  
Göteborg, Sweden 2011

Development of an ASPEN Plus model of a Chemical-looping reformer reactor  
Master's Thesis  
DANIEL CHRISTOPH FERNADNES LOHSE

© DANIEL CHRISTOPH FERNANDES LOHSE, 2011

Master's Thesis 2011: T2011-362  
Department of Energy and Environment  
Division of Energy Technology

Chalmers University of Technology  
SE-412 96 Göteborg  
Sweden  
Telephone: + 46 (0)31-772 1000

Cover:  
Figure text for the cover picture (if applicable), possibly with reference to more extensive information in the report.

Chalmers Reproservice  
Göteborg, Sweden 2011

## Development of an ASPEN plus model of a Chemical-looping reformer reactor

DANIEL CHRISTOPH FERNANDES LOHSE  
Department of Energy and Environment  
Division of Energy Technology  
Chalmers University of Technology  
SE-412 96 Göteborg (Sweden)

### ABSTRACT

Synthetic Natural Gas (SNG) from biomass gasification is viewed as a promising option for production of transport fuels. A major problem associated is the removal of contaminants derived from the gasification step, such as tars. Tars are aromatic compounds, usually between 1 and 5 rings, which at 350°C already start to condensate, causing clogging and blockage of components. Catalytic tar conversion presents advantages compared to other technologies and in particular it allows thermal integration with the gasification step, lowering the thermodynamic losses, and enables the use of the energy contained in the tars by converting them into usable gases, such as H<sub>2</sub> and CO. Catalyst deactivation can be caused by coke deposits. A novel technique named Chemical-looping reforming (CLR), based on Chemical-looping combustion concept (CLC), is being developed in Chalmers University of Technology to tackle this problem. It is based in a two reactor system, one Fuel reactor (FR) and an Air reactor (AR). In the FR the tars are oxidized due to the reduction of the catalyst. In the AR the catalyst is newly oxidized and the coke deposits are combusted.

The present work intends to analyze raw data, measured from a bench-size CLR facility using different catalysts and O<sub>2</sub> concentrations in the AR, in order to elaborate a descriptive model of the system in order to assess how the reforming step influences the fate of the incondensable gases (H<sub>2</sub>, CO, CO<sub>2</sub>, CH<sub>4</sub>, C<sub>2</sub>H<sub>2</sub>, C<sub>2</sub>H<sub>4</sub>, C<sub>2</sub>H<sub>6</sub>, C<sub>3</sub>H<sub>8</sub>, and N<sub>2</sub>) This is achieved by firstly elaborating a molar balance to both reactors taking into account the system main constituents (Carbon, Oxygen, Hydrogen and Nitrogen) and afterwards implementing it in Matlab, in order to solve the balance. The model was elaborated using commercial flow-sheet software called Aspen Plus.

**KEYWORDS:** biomass, synthetic natural gas, tar, incondensable gases, chemical-looping reforming, molar balance, Aspen plus

# ACKNOWLEDGMENTS

It is a pleasure to thank those who made this thesis possible.

My coordinators Nicolas Berguerand and Martin Seeman, who guided me through this work.

Phd Students Stefan Heyne and Fredrik Lind, for their valuable inputs, advices and knowledge provided.

Department of Energy and Environment at the Chalmers University of Technology which provided me with great working conditions, friendly colleagues and tasty fikas.

My working colleague Maria Inês, who helped me finding this Master Thesis and was always open to discuss problems related with the work.

My parents, Luísa and Matthias, for all the emotional and financial support. Not only during this Erasmus year in Sweden but also through all my (still short) life and academic path. A very big, THANK YOU!

My aunt Fernanda, for all the support as well.

Tobias, who has always been a great brother and put up with me since the beginning.

All my family in Portugal, Germany and Japan.

My friends in Portugal.

My not only friends but also study colleagues. All the long working hours I spent in university were much easier to overcome due to all the laughter and good moments I shared with you during these 5 years.

At last but not least, all the friends I made in Göteborg throughout this Erasmus year: the ghettos, Frölunda neighbors, flatmates, etc., you were the ones who made this experience truly amazing and worth remembering.

To all of you,

THANK YOU!

# Contents

|   |    |
|---|----|
| ABSTRACT .....  | 5  |
| ACKNOWLEDGMENTS .....   | 6  |
| 1. Introduction.....  | 14 |
| 1.1. Background .....   | 14 |
| 1.2. Aim and scope.....   | 15 |
| 1.3. Thesis outline .....                                       | 16 |
| 2. Theory .....   | 17 |
| 2.1. Gasification.....  | 17 |
| 2.2. Methanation.....   | 18 |
| 2.3. Chemical Looping Reforming .....                           | 18 |
| 2.4. Aspen Plus .....   | 21 |
| 3. Experimental .....   | 24 |
| 3.1. CLR system, components and flows .....                     | 24 |
| 3.2. Measurements.....  | 27 |
| 3.3. Operational conditions and data used .....                 | 29 |
| 4. Methodology.....   | 30 |
| 4.1. Variables overview .....                                   | 30 |
| 4.2. Molar balance calculations .....                           | 31 |
| 4.3. Molar balance.....   | 35 |
| 4.4. MatLab implementation .....                                | 37 |
| 4.5. Aspen Plus .....   | 38 |
| 4.6. Energetic assessment .....                                 | 41 |
| 5. Results and discussion.....                                  | 43 |
| 5.1. Molar balance.....   | 43 |
| 5.1.1. 60% Ilmenite / 40% Silica-sand and 1% oxygen in AR ..... | 43 |
| 5.1.2. 23% Manganese / 77% Silica-sand at 800°C.....            | 46 |
| 5.2. Data analysis.....   | 47 |
| 5.2.1. 60% Ilmenite / 40% Silica-sand and 1% oxygen in AR ..... | 48 |
| 5.2.2. 23% Manganese / 77% Silica-sand at 800°C.....            | 50 |
| 5.3. Aspen and balance comparison .....                         | 53 |
| 5.3.1. 60% Ilmenite, 40% Silica-sand and 1% oxygen in AR .....  | 53 |
| 5.4. Energetic assessment .....                                 | 58 |

|   |    |
|---|----|
| 6. Conclusion.....  | 60 |
| Further works .....   | 61 |
| Bibliography.....   | 62 |
| Appendix I – Old Aspen Plus CLR flow-sheet.....                       | 65 |
| Appendix II – MatLab file for molar balance.....                      | 66 |
| Appendix III – MatLab input Excel file examples .....                 | 72 |
| Appendix IV – MatLab results example .....                            | 75 |
| Appendix V – Sensitivity analysis .....                               | 76 |
| Appendix VI – New Aspen Plus CLR flow-sheet with tested reactors..... | 81 |
| Appendix VII – Molar balance values for ASPEN input data.....         | 82 |

# Table of Figures

|   |    |
|---|----|
| FIGURE 1 - GENERAL PROCESS STEPS TO PRODUCE SNG BY THERMAL GASIFICATION OF BIOMASS (5) .....                            | 14 |
| FIGURE 2 - CLR LOCATION IN PRODUCTION PROCESS .....   | 17 |
| FIGURE 3 - TYPICAL GAS COMPOSITION AT THE EXHAUST OF THE GASIFIER (DRY BASIS) AND CORRESPONDING HEAT CONTENT (22) ..... | 18 |
| FIGURE 4 - SCHEMATIC FLOWCHART OF THE CLR (5).....  | 19 |
| FIGURE 5 – DEFAULT ASPEN PLUS GIBBS REACTOR .....   | 22 |
| FIGURE 6 – DEFAULT ASPEN PLUS EQUILIBRIUM REACTOR.....  | 22 |
| FIGURE 7 – DEFAULT ASPEN PLUS PLUG FLOW REACTOR .....   | 23 |
| FIGURE 8 - CLR SYSTEM .....   | 25 |
| FIGURE 9 - - EXPERIMENTAL SETUP SCHEME (27) .....   | 27 |
| FIGURE 10 - TWO OF THE THREE GAS ANALYZING SETUPS.....  | 28 |
| FIGURE 11 - MOLAR BALANCE SYSTEM STREAMS OVERVIEW .....   | 32 |
| FIGURE 12 - MATLAB SCHEME.....  | 37 |
| FIGURE 13 - IN AND OUTLET FLOW SCHEME IN ASPEN MODEL .....  | 39 |
| FIGURE 14 - TEMPERATURE APPROACH SCHEME .....   | 40 |
| FIGURE 15 - ENERGY ASSESSMENT SCHEME .....  | 41 |
| FIGURE 16 - GRAPH LABEL.....  | 47 |
| FIGURE 17 - HYDROGEN FR OUT SENSITIVITY ANALYSIS .....  | 48 |
| FIGURE 18 - HYDROGEN FR IN SENSITIVITY ANALYSIS .....   | 48 |
| FIGURE 19 - CARBON MONOXIDE FR OUT SENSITIVITY ANALYSIS .....   | 48 |
| FIGURE 20 - CARBON MONOXIDE FR IN SENSITIVITY ANALYSIS.....   | 48 |
| FIGURE 21 - NITROGEN FR OUT SENSITIVITY ANALYSIS .....  | 49 |
| FIGURE 22 - NITROGEN FR IN SENSITIVITY ANALYSIS .....   | 49 |
| FIGURE 23 - CARBON DIOXIDE FR OUT SENSITIVITY ANALYSIS .....  | 49 |
| FIGURE 24 - OXYGEN AR OUT SENSITIVITY ANALYSIS .....  | 49 |
| FIGURE 25 - DRY FLOW FR OUT SENSITIVITY ANALYSIS .....  | 49 |
| FIGURE 26 - WATER FR IN SENSITIVITY ANALYSIS .....  | 49 |
| FIGURE 27 - HYDROGEN FR OUT SENSITIVITY ANALYSIS .....  | 51 |
| FIGURE 28 - HYDROGEN FR IN SENSITIVITY ANALYSIS .....   | 51 |
| FIGURE 29 - CARBON MONOXIDE FR OUT SENSITIVITY ANALYSIS .....   | 51 |

|  |    |
|--|----|
| FIGURE 30 - CARBON MONOXIDE FR IN SENSITIVITY ANALYSIS.....  | 51 |
| FIGURE 31 - NITROGEN FR OUT SENSITIVITY ANALYSIS .....       | 51 |
| FIGURE 32 - NITROGEN FR IN SENSITIVITY ANALYSIS .....        | 51 |
| FIGURE 33 - CARBON DIOXIDE AR OUT SENSITIVITY ANALYSIS ..... | 52 |
| FIGURE 34 - OXYGEN AR OUT SENSITIVITY ANALYSIS .....         | 52 |
| FIGURE 35 - DRY FLOW FR OUT SENSITIVITY ANALYSIS .....       | 52 |
| FIGURE 36 - WATER FR IN SENSITIVITY ANALYSIS .....           | 52 |

## Table of Equations

|   |    |
|---|----|
| EQUATION 1 – METHANATION REACTION .....                         | 18 |
| EQUATION 2 - PARTIAL OXIDATION OF THE TAR (8) .....             | 19 |
| EQUATION 3 - CATALYST RE-OXIDATION AND COKE OXIDATION (8) ..... | 19 |
| EQUATION 4 - STEAM REFORMING .....                              | 20 |
| EQUATION 5 - STEAM DEALKYLATION .....                           | 20 |
| EQUATION 6 - HYDRO CRACKING .....                               | 20 |
| EQUATION 7 - HYDRO DEALKYLATION .....                           | 20 |
| EQUATION 8 - DRY REFORMING .....                                | 20 |
| EQUATION 9 – CRACKING .....                                     | 20 |
| EQUATION 10 – CARBON FORMATION .....                            | 20 |
| EQUATION 11 – WATER-GAS SHIFT .....                             | 21 |
| EQUATION 12 - METHANATION .....                                 | 21 |
| EQUATION 13 - METHANATION .....                                 | 21 |
| EQUATION 14 – WATER GAS .....                                   | 21 |
| EQUATION 15 – WATER GAS .....                                   | 21 |
| EQUATION 16 - BOUDOUARD .....                                   | 21 |
| EQUATION 17- GENERAL POWER-LAW EQUATION .....                   | 23 |
| EQUATION 18 - N2 CORRECTION .....                               | 32 |
| EQUATION 19 - ELEMENT (Xi) CORRECTION.....                      | 33 |
| EQUATION 20- ELEMENT (Xi) NORMALIZATION .....                   | 33 |
| EQUATION 21 - HELIUM CONCENTRATION .....                        | 33 |
| EQUATION 22- CARBON BALANCE .....                               | 35 |
| EQUATION 23 - HYDROGEN BALANCE.....                             | 35 |

|   |    |
|---|----|
| EQUATION 24 - OXYGEN BALANCE .....  | 35 |
| EQUATION 25 - NITROGEN BALANCE .....  | 36 |
| EQUATION 26 - NITROGEN OUT OF AR, FUNCTION OF THE BALANCE .....               | 36 |
| EQUATION 27 - NITROGEN OUT OF AR, FUNCTION OF THE HELIUM BALANCE .....        | 36 |
| EQUATION 28 - NITROGEN BALANCE RESIDUE SIGMA IN (%) .....                     | 36 |
| EQUATION 29 - AR FLOW VARIATION IN (%).....                                   | 37 |
| EQUATION 30 - N <sub>2</sub> FR FLOW VARIATION IN (%).....                    | 37 |
| EQUATION 31 - COMBUSTION HEAT CHANGE BETWEEN IN AND OUTLET GASES IN (%) ..... | 41 |

## Table of Tables

|  |    |
|--|----|
| TABLE 1 – TAR REFORMING REACTIONS .....  | 20 |
| TABLE 2 - EQUILIBRIUM REACTION .....   | 21 |
| TABLE 3 - GEOMETRICAL SIZES OF THE CLR-SYSTEM .....                                | 26 |
| TABLE 4 - GAS ANALYZING INSTRUMENTS DOWNSTREAM OF THE AR.....                      | 26 |
| TABLE 5 - SYSTEM CONDITIONS FROM THE USED RAW DATA.....                            | 29 |
| TABLE 6 - POWER LAW DATA FOR NAPHTHALENE (9) .....                                 | 29 |
| TABLE 7 - VARIABLE OVERVIEW .....  | 31 |
| TABLE 8 - FLOWS CALCULATION FORMULAS .....   | 39 |
| TABLE 9 - MOLAR BALANCE RESULTS .....  | 44 |
| TABLE 10 - RESULTS VARIATION .....   | 44 |
| TABLE 11 - CANDIDATE DATA FOR ASPEN PLUS .....                                     | 45 |
| TABLE 12 - MOLAR BALANCE RESULTS .....   | 46 |
| TABLE 13 - RESULTS VARIATION .....   | 47 |
| TABLE 14 - COMPONENT MOLAR FR BALANCE RESULTS .....                                | 53 |
| TABLE 15 - GIBBS REACTOR RESULTS .....   | 54 |
| TABLE 16 - EQUILIBRIUM REACTOR RESULTS WITHOUT TEMPERATURE APPROACH .....          | 55 |
| TABLE 17 - EQUILIBRIUM REACTOR RESULTS WITH TEMPERATURE APPROACH .....             | 56 |
| TABLE 18 - PLUG FLOW REACTOR WITH NAPHTHALENE POWER LAW VALUES .....               | 57 |
| TABLE 19 - PLUG FLOW REACTOR WITH $K_{TARS}$ FOUND THROUGH ITERATIVE PROCESS ..... | 58 |
| TABLE 20 - CHEMICAL ENERGY LOSS ASSESSMENT .....                                   | 59 |

# Abbreviations and Nomenclature

## Abbreviations

|      |                                   |
|------|-----------------------------------|
| CCS  | -Carbon Capture and Storage       |
| SNG  | -Synthetic Natural Gas            |
| CHP  | -Combined Heat and Power          |
| CLR  | -Chemical Looping Reforming       |
| FR   | -Fuel Reactor                     |
| AR   | -Air Reactor                      |
| LS   | -Loop-Seal                        |
| SLS  | -Superior Loop-Seal               |
| ILS  | -Inferior Loop-Seal               |
| GC   | -Gas Chromatography               |
| SPA  | -Solid Phase Adsorption           |
| NDIR | -Non Dispersive Infrared Analyzer |
| MeO  | -Metal Oxide                      |

## Nomenclature

| Formula symbol       | Unit              | Definition                 |
|----------------------|-------------------|----------------------------|
| $\Delta H_r^{298 K}$ | $[kJ/mol]$        | Reaction enthalpy at 298 K |
| $Me_xO_y$            | $[-]$             | Reduced metal oxide        |
| $Me_xO_{y-1}$        | $[-]$             | Oxidized metal oxide       |
| $r$                  | $[mol/L \cdot s]$ | Rate of reaction           |
| $T$                  | $[K]$             | Reactor temperature        |
| $n$                  | $[-]$             | Temperature exponent       |
| $E$                  | $[kJ/mol]$        | Activation energy          |

|   |               |   |
|---|---------------|---|
| $R$                                     | $[kJ/mol.K]$  | Gas law constant  |
| $C_i$                                   | $[mol/L]$     | Molar concentration of the component i  |
| $\alpha_i$                              | $[-]$         | Exponent of the component i   |
| $k$                                     | <i>varies</i> | Pre-exponential factor  |
| $[X_i]$                                 | $[%]$         | Volumetric concentration of the component i   |
| $g_{tars}$                              | $[g/L]$       | Tar concentration   |
| $w_{in}$                                | $[g/L]$       | H <sub>2</sub> O concentration  |
| $\dot{n}$                               | $[mol/min]$   | Molar flow  |
| $M_i$                                   | $[g/mole]$    | Molar mass of the component i   |
| $V_m$                                   | $[L/mol]$     | Molar volume  |
| $\sigma$                                | $[%]$         | Residue   |
| $\Delta_{balance}$                      | $[%]$         | Molar balance component variation   |
| $\Delta_{Gibbs}$                        | $[%]$         | Gibbs reactor component variation   |
| $\Delta_{Eq.}$                          | $[%]$         | Equilibrium reactor component variation   |
| $\Delta_{T.app.}$                       | $[%]$         | Temperature approach component variation  |
| $\Delta_{k_{C_8H_{10}}}$                | $[%]$         | Naphthalene power law component variation   |
| $\Delta_{k_{iter.}}$                    | $[%]$         | Chemical constant (Iteratively calculated to match outlet tar flow) component variation |
| $\Delta H_{C_{inlet\ gases}}^{298\ K}$  | $[kJ/mol]$    | Combustion heat for fuel reactor inlet gases  |
| $\Delta H_{C_{outlet\ gases}}^{298\ K}$ | $[kJ/mol]$    | Combustion heat for fuel reactor outlet gases   |
| $\Delta \dot{n}_{AR}$                   | $[%]$         | Air reactor flow change   |
| $\Delta \dot{n}_{FR}^{N_2}$             | $[%]$         | Air reactor nitrogen flow change  |

# 1. Introduction

## 1.1. Background

As a result of human activities and in particular the energy conversion by processing fossil fuels, there has been an almost unfettered release of greenhouse gases in the atmosphere, leading to the more general climate change patterns we are now witnessing. Meanwhile, fuel prices are nearly constantly rising (1). Thus, focus on sustainable energy forms like solar, hydropower, wind, biomass (2) and other technologies has increased, abating these emissions. Out of these alternatives, using biomass as feedstock has emerged as an appealing compromise since the combustion process itself does not contribute to a net increase in the atmospheric CO<sub>2</sub> (3). Indeed, the associated emissions are compensated by the uptake through biomass growth. If Carbon capture and storage (CCS) is included, it can even lead to a net decrease of carbon dioxide. For these reasons in particular, the worldwide interest in biomass related technologies has been increasing (4). It is regarded as the renewable energy source with the highest potential to fulfill the energy demands of modern society (2).

Regarding the transport fuels, Synthetic Natural Gas (SNG) from biomass is seen as a promising option. The integration of SNG production with combined heat and power (CHP) plants is proven to be an efficient way of converting excess heat from the production line to electricity (5).



Figure 1 - General process steps to produce SNG by thermal gasification of biomass (5)

The biggest obstacles to overcome in order to make SNG viable is the elimination of existing contaminants/impurities, derived from the gasification step, such as tars and contaminants containing nitrogen, sulfur and chlorine. In other words, a major goal is to achieve the reduction of the concentration of these components in order to meet environmental and health standards and become compatible with the end use application (6). Nevertheless, one of the most important problems is the tar removal/elimination (7).

Tars are a mix of aromatic compounds, usually between 1 and 5 rings, with hydrocarbons containing oxygen and sulfur. At 350°C some already start to condensate, causing clogging and blockage of components (8), leading to the decrease of total efficiency and an increase in costs (9).

In order to eliminate the tars from the gas, several processes with different principles exist:

- Physical process, such as wet and wet-dry gas cleaning consisting mainly on temperature reduction, tar condensation and following separation (10);
- Thermal, Steam and Oxidative conversion (10);
- Catalytic destruction and conversion (10).

High temperature process, that is 2<sup>nd</sup> and 3<sup>rd</sup> in the list above, are preferred, as the thermodynamic losses are lower, while being higher if gas cooling is taken into consideration (8).

The catalytic processes are divided into primary and secondary tar cleaning. By primary is meant that a catalyst is added as bed material still in the gasification step while secondary cleaning is performed by treating the gas only after. The latter is generally preferred due to the optimization possibility with respect to tar removal is higher (8). Tars are as well most often associated with catalyst deactivation, since coke formation, originated from the conversion reaction, deposit on the catalyst's surface.

An innovative concept to tackle this problem is being developed in Chalmers University of Technology (8). It is referred to as Chemical Looping Reforming (CLR). The principle is based on a two reactor system, a Fuel Reactor (FR) and an Air Reactor (AR). In the FR the tars are reformed and the AR is used to regenerate the catalyst. Recent experiment using the CLR system provided initial results supporting the feasibility of such a tar removal process (8). The purpose of this thesis is to analyze the complete raw data set obtained from these experiments and improve a simplified model in Aspen Plus describing the system.

## 1.2. Aim and scope

This thesis has the objective to improve an existing model of the CLR reactor (Appendix I ) which is part of a process model describing the production of SNG. Based on the available raw data, semi-kinetic expressions can be derived to describe the fate of the incondensable gases ( $H_2$ ,  $CO$ ,  $CO_2$ ,  $CH_4$ ,  $C_2H_2$ ,  $C_2H_4$ ,  $C_2H_6$ ,  $C_3H_8$ , and  $N_2$ ). These expressions will be implemented in the Aspen Plus model. It is important to mention that this master thesis will not focus specifically on the Tar destruction, as this will be handled in another dissertation. More focus is given on the non-condensable gases while for the tars is considered a simple/global conversion model that can keep track of temperature or oxygen concentrations. Also important to mention is that the raw data was not obtained in the scope of this work but was in fact provided.

All the measurements and following data obtained were neither obtained in the ambit of this thesis nor were the measurements made by the author of this report.

### **1.3. Thesis outline**

In first part, a broader approach is made to contextualize the system in the already existing gas processing technologies and to explain in which way the CLR can tackle problems that usually are a barrier to catalytically reform the tar.

Then is presented all the theory related to the system, such as relevant chemical equations, up and downstream processes and how the two reactor system should theoretically operate.

All the experimental facilities' characteristics, measurement methods and raw data provided are presented in the 3<sup>rd</sup> section

Methodology is explained in section 4, completed with relevant comments to all the data, simplifications and assumptions made.

All results and associated discussion are in section 5.

Finally, all conclusions and subjects to further investigation are referred in the last part.

## 2. Theory

This section includes all the aspects regarding the CLR. Moreover, up and downstream system characteristics, gasifier and methanation steps respectively are also mentioned in order to better understand the requirements relatively to the tar reforming step. Fig. 2 shows a flow-sheet where the CLR is integrated in the SNG process.

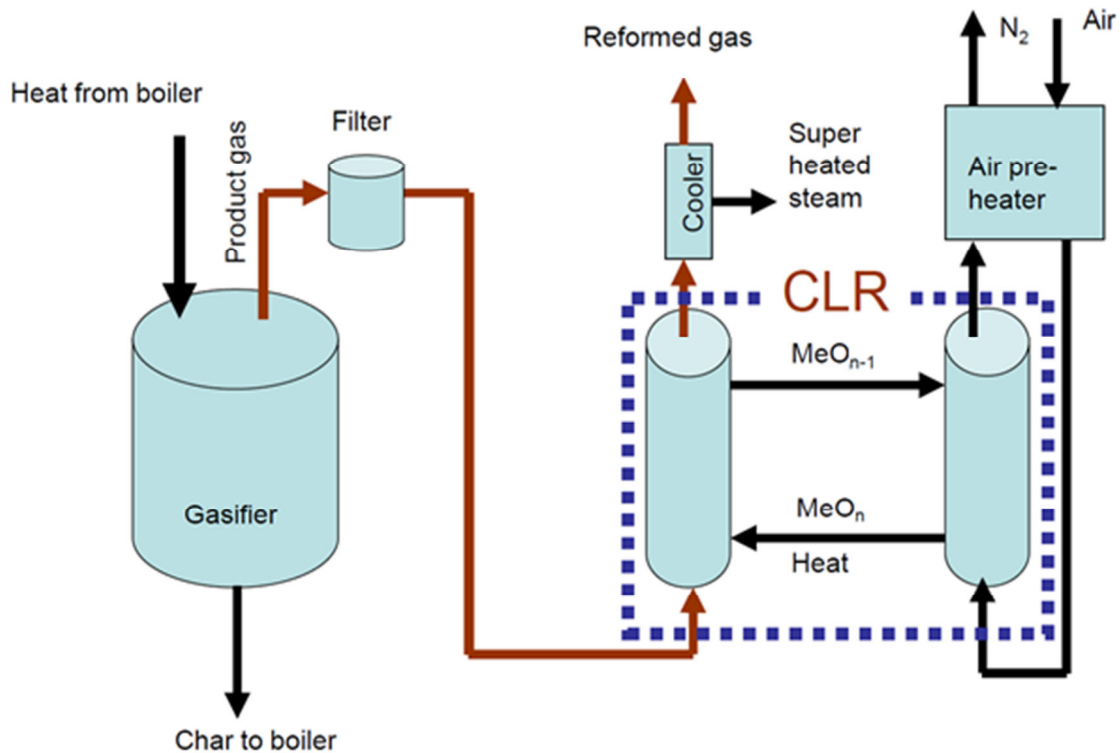


Figure 2 - CLR location in production process

### 2.1. Gasification

During experiment, the CLR was fed with a stream of crude gas from the Chalmers 2-4 MW<sub>th</sub> indirect gasifier operated with biomass. A typical gas molar constitution is presented in Fig. 3 below:

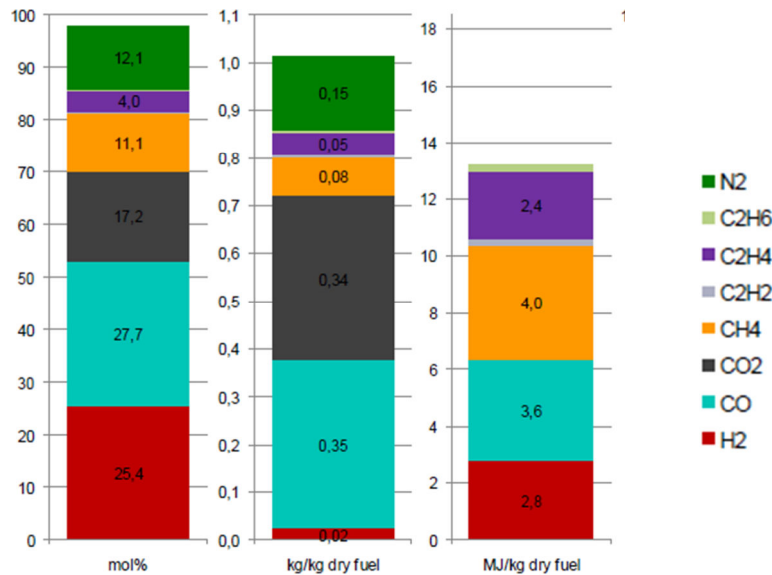


Figure 3 - Typical gas composition at the exhaust of the gasifier (dry basis) and corresponding heat content (22)

## 2.2. Methanation

The methanation consists in the conversion of the reformed gas to methane. The most important reaction occurring in this step is stated in e.g. (11) and reads:



### Equation 1 – Methanation reaction

In particular, equation 1 shows how the hydrogen to carbon monoxide molar relation is 3/1. In other words, the gas to be processed during methanation shall preferably have a ratio H<sub>2</sub>/CO close to 3. As shown in Fig.2, the raw gas has a ratio around 0,8.

## 2.3. Chemical Looping Reforming

Physical processes for tar removal consist in a gas temperature reduction, leading to tar condensation and enabling its removal. To this kind of removal is associated a thermal penalty and waste water/solvents as well.

However, catalytic hot gas cleaning processes are viewed as promising. They can be divided into two groups, primary and secondary. A primary process consist in adding catalyst already in the gasification step but secondary cleaning, which consist in performing removal after the gasification step, is usually preferred, as it gives better optimizations possibilities towards tar removal (8). In different catalytic conversion methods, with one reactor operated as a fixed bed carbon particles are likely to deposit on the catalyst, provoking its deactivation. In a fixed bed, only tar concentrations up to 2 g<sub>tar</sub>/Nm<sup>3</sup> could be tolerated while in a fluidized bed, the concentrations can reach as high values as e.g. 43 g<sub>tar</sub>/Nm<sup>3</sup> (12). An innovative concept based on a two reactor tar cleaning system is being developed in Chalmers University of Technology to tackle this problem.

The main benefit from the double reactor system relies on the existence of two separate reactors. In this way, direct contact between the gas and air is avoided, preventing nitrogen dilution (8). Another clear advantage of this system is the removal from char deposits on the catalyst, which form during the tar oxidation.

In the CLR concept, a Metal oxide (MeO) works as an oxygen transporter and heat carrier for the tar oxidation reactions in the FR (8) without the need of an additional heat source. Once reduced, it returns to the AR to again be oxidized. The oxidized form of the catalyst is represented by  $Me_xO_y$  while the reduced form by  $Me_xO_{y-1}$ .

Fig. 4 below represents the general functioning of the CLR system:

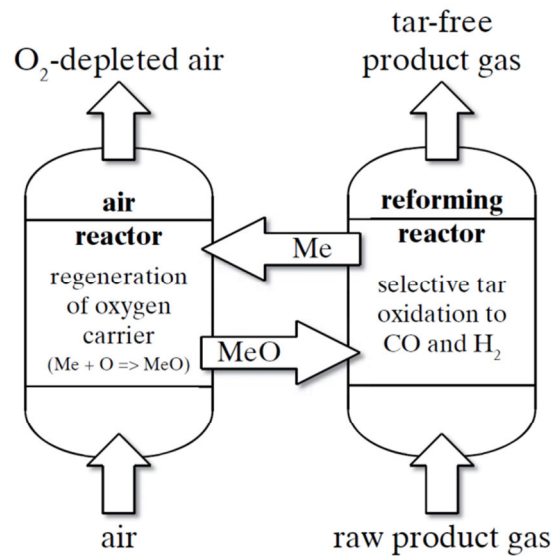
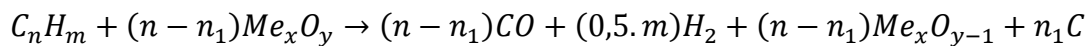


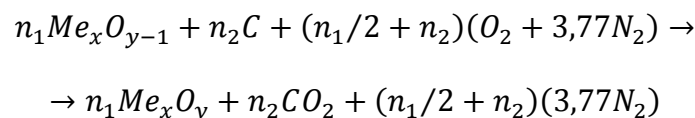
Figure 4 - Schematic flowchart of the CLR (5)

Inside the FR, the tars, represented by the general formula  $C_nH_m$ , are oxidized according to the reaction:



Equation 2 - Partial oxidation of the tar (8)

On the other hand, the oxygen carrier is re-oxidized in the AR according to:



Equation 3 - Catalyst re-oxidation and coke oxidation (8)

The reaction in the AR is exothermic. So, the heat carry properties from the catalyst can be used to provide energy for the generally endothermic reaction happening in the FR.

Catalytic tar breakdown is still surrounded by a high complexity. However, previous investigations were able to provide a list of reaction that possibly could occur in the reactor (8).

**Table 1 – Tar reforming reactions**

|                                 |  |
|---------------------------------|--|
|                                 | $C_nH_m + nH_2O \rightarrow nCO + (n + 0,5m)H_2$     |
| Equation 4 - Steam reforming    |  |
|                                 | $C_nH_m + xH_2O \rightarrow C_iH_j + pH_2 + qCO$     |
| Equation 5 - Steam dealkylation |  |
|                                 | $C_nH_m + (2n - (m/2))H_2 \rightarrow nCH_4$         |
| Equation 6 - Hydro cracking     |  |
|                                 | $C_nH_m + xH_2 \rightarrow C_iH_j + qCH_4$           |
| Equation 7 - Hydro dealkylation |  |
|                                 | $C_nH_m + nCO_2 \rightarrow 2nCO + 0,5mH_2$          |
| Equation 8 - Dry reforming      |  |
|                                 | $C_nH_{2(n+1)} \rightarrow C_{n-1}H_{2(n-1)} + CH_4$ |
| Equation 9 – Cracking           |  |
|                                 | $C_nH_{2(n+1)} \rightarrow nC + (n + 1)H_2$          |
| Equation 10 – Carbon formation  |  |

These are derived from earlier research using toluene as a tar component but these equations are presented in a general way, as different formulas exist. The majority of the proposed equation (4-8 and 10) were obtained from (13) while number 9 from (14).

On top of the aforementioned tar removal reactions, several equilibrium reactions could be involved. Table 2 summarizes the most relevant ones.

Table 2 - Equilibrium reaction

|                               |   |
|-------------------------------|---|
|                               | $CO + H_2O \leftrightarrow H_2 + CO_2$  |
| Equation 11 – Water-gas shift |   |
|                               | $CO + 3H_2 \leftrightarrow CH_4 + H_2O$ |
| Equation 12 – Methanation     |   |
|                               | $2H_2 + C \leftrightarrow CH_4$         |
| Equation 13 – Methanation     |   |
|                               | $CO + 2H_2 \leftrightarrow H_2O + C$    |
| Equation 14 – Water gas       |   |
|                               | $CO_2 + 2H_2 \leftrightarrow 2H_2O + C$ |
| Equation 15 – Water gas       |   |
|                               | $C + CO \leftrightarrow 2CO$            |
| Equation 16 – Boudouard       |   |

Some reactions are favored by specific catalysts.

## 2.4. Aspen Plus

In order to understand the computational part of this thesis, a summarizing description of the used software tools is given, to enable a better understanding of the process applied. Only the software's main functionalities are described.

Aspen Plus is a process simulation software which uses "basic engineering relationships, such as mass and energy balances, and phase and chemical equilibrium" (15).

It consists in flow sheet simulations that calculate stream flow rates, compositions, properties and also operation conditions.

The main focus is on the reactors used in the attempt to model the CLR.

### Gibbs Reactor

Calculations are done based on Gibbs free energy concepts (16). Product gas has a composition so that the Gibbs free energy is at a minimum. At least two reactor conditions have to be defined, e.g. Temperature and Pressure. Fig.5 below shows the representation of such a reactor in ASPEN.

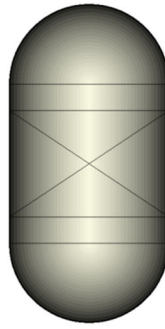


Figure 5 – Default Aspen Plus Gibbs reactor

### Equilibrium reactor

Similar to the Gibbs reactor, in this case equilibrium concentrations are calculated. The difference relies on the fact that the equilibrium is only calculated for given reactions. These have to be specified. So, only specific components will suffer chemical transformation, while the components for which no equations were defined, remain unaltered. Fig.6 shows such a reactor in ASPEN.

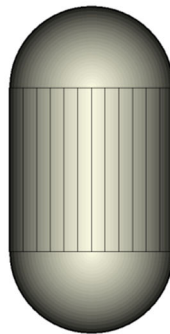


Figure 6 – Default Aspen Plus Equilibrium reactor

A characteristic of this reactor is the temperature approach for a specific equation. It is related to a reactor option in ASPEN that gives the possibility to change the temperature and consequentially the equilibrium at which a specific reaction should be calculated. Normally, a general reactor temperature is introduced but this option gives the possibility to change the final compound constitution, enabling to adjust outlet gas concentrations in order to fit for e.g. software results with experimental data. One drawback of this reactor is that it does not allow reactor optimization and modeling because the reaction kinetics are not taken into account. However, this still gives information about the energy involved in the reactions.

### Plug flow reactor

In this kind of reactor, reaction kinetic needs to be specified and, in actual modeling, the power-law is used. A general power-law representation is given as:

$$r = kT^n e^{-(E/TR)} \prod_{i=1}^N C_i^{\alpha_i}$$

**Equation 17- General power-law equation**

A representation of such a reactor in ASPEN is in Fig.7.

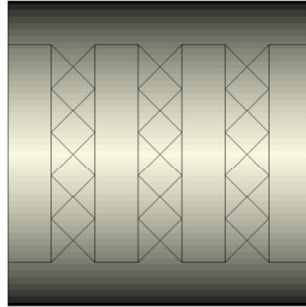


**Figure 7 – Default Aspen Plus Plug flow reactor**

As dynamics are included it is possible to extract information for reactor modeling and further optimization. E.g., assessing how the residence time influences the tar breakdown in order to check the CLR system dimensions needed for complete tar breakdown.

Aspen Plus has a larger selection of reactor models than the ones presented before. However, for a first try approach, the three mentioned were used. In the following, both advantages and drawbacks are presented:

- Gibbs and Equilibrium reactors
  - Easy to use and good for including in larger simulations/system studies;
  - No predictions/guidance of experiments possible.
  
- Plug flow reactor
  - Reaction kinetics and residence time involved, which can be used to guide the experiments;
  - More complex.

## 3. Experimental

This chapter focuses on describing the system in general approach, providing features necessary to understand the data evaluation and following discussion. It includes in particular, all the components, flows, measurements and measurement tools used in the assessments. Note that, here, the CLR is a bench-scale system not self-supporting in energy and thus, heat requirements are ensured via an oven.

### 3.1. CLR system, components and flows

The main part of the CLR system consists of two separate reactors, the FR and the AR. Both are connected via two loop seals, the Superior Loop-Seal (SLS) and the Inferior Loop-Seal (ILS). Through the ILS the reduced catalyst passes from the FR to the AR while the SLS is used to transport the oxidized catalyst from the AR to the FR. The FR is designed as a bubbling fluidized bed to “enable calculations of the gas/solid contact” (8) while the AR is designed as a circulating fluidized bed. Both reactors are surrounded by a two-pieced ove, offering the possibility to heat the parts separately. Besides, the air cooling jacket is welded on the FR, enabling operation temperatures differences up to 200°C between the reactors. The system is operated at a sub-atmosphere pressure between -4 and -6 kPa due to security reasons related to the gasifier operation and the pressure between both reactors is kept around 500 Pa to prevent leakages. Fig.8 shows the reactor system and the surrounding oven on the rails.



Figure 8 - CLR system

All gases entering and fluidizing the beds in the reactor system pass through wind boxes and via porous plates, in order to reduce pressure variations. In total, seven flows of gases and solids are involved in the system:

- Raw gas produced in the gasifier entering the CLR system through the FR;
- Reformed gas leaving the CLR system out of the FR;
- Nitrogen/Air mixture entering the CLR system through the AR;
- Gas leaving the CLR system from the AR;
- Two individual helium flows, used to fluidize the loop seals;
- Catalyst flows between the reactors.

The raw gas line is heated to approximately 400°C to prevent tar condensation. Upstream the FR wind-box, a T-connection enables inert operation with nitrogen prior to raw gas addition itself. An also vital part of the system important to mention is how the raw gases are introduced in the FR. As upstream from the reactors the gases are too hot, they cannot be pumped into the FR reactor so, the pump is located downstream of the reactor and the gas cleaning process and upstream from the gas measurement tools.

At the AR inlet, the air/nitrogen mixture is pre-heated. Both flows, Nitrogen and Air, are controlled separately, permitting O<sub>2</sub> concentration control.

Two separately controlled helium flows allow independent fluidization of ILS and SLS.

The exhaust gas stream from the AR passes through a cyclone, removing entrained catalyst and recycles it back to the FR. Tables 3 and 4 display geometric dimensions and AR concentration measurement device characteristics, respectively, while Fig.9 shows a draft of the whole system and measurement devices.

**Table 3 - Geometrical sizes of the CLR-system**

|                                 | <b>Cross-sectional (mm)</b> | <b>Height (mm)</b> |
|---------------------------------|-----------------------------|--------------------|
| <b>Fuel reactor (FR)</b>        | 50 x 50                     | 380                |
| <b>Air reactor (AR)</b>         | 20 x 20                     | 460                |
| <b>Superior loop seal (SLS)</b> | 23 x 23                     | 120                |
| <b>Inferior loop seal (ILS)</b> | 23 x 23                     | 50                 |

**Table 4 - Gas analyzing instruments downstream of the AR**

| <b>Instrument</b>     | <b>Measuring interval (Mole %)</b> | <b>Detection limit (ppm)</b> |
|-----------------------|------------------------------------|------------------------------|
| <b>O<sub>2</sub></b>  | 0 – 25                             | 1250                         |
| <b>CO</b>             | 0 – 1                              | 50                           |
| <b>CO<sub>2</sub></b> | 0 – 100                            | 5000                         |

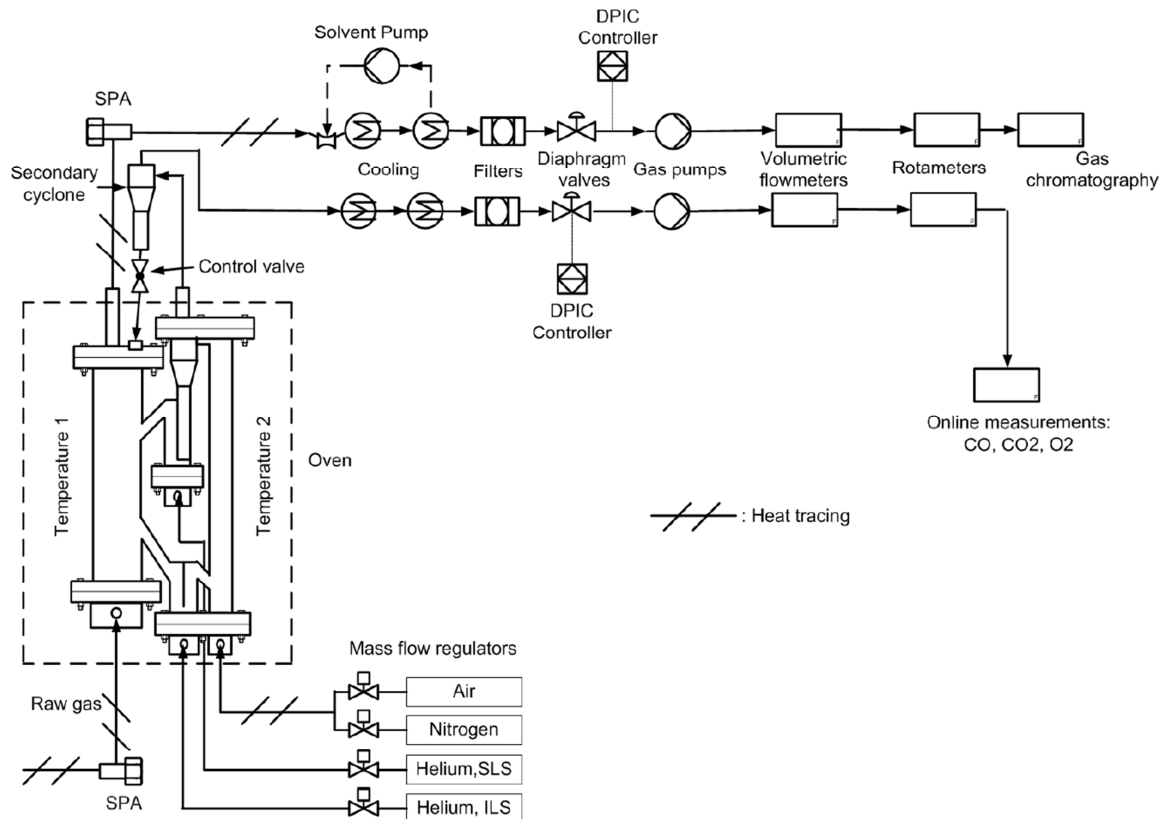


Figure 9 -- Experimental setup scheme (27)

### 3.2. Measurements

Pressure and temperature measurements were made with 10 pressure tabs, inclined 45° to prevent particles from blocking, and 10 thermocouples.

The gas stream, from the gasifier and leaving the FR, are measured using the same procedure. Gas streams, total flow in the case of reformed gas and sample flows regarding the gasifier gas, is mixed with iso-propanol, dissolving the remaining tar components, also protecting the downstream equipment from fouling. This mixture is cooled and the condensate is separate by gravity. The iso-propanol is then recirculated back, continuing to be used as a solvent for the tars. An additional cooling and drying step using a Peltier cooler is included for the gas. Possible remaining moisture is removed using silica gel. Finally, the gas passes through a volumetric membrane flow meter and a rotameter and its composition is measured at the end with the Micro-Gas Chromatography (GC). A picture of the measuring facilities is shown in Fig.10.



Figure 10 - Two of the three gas analyzing setups

Regarding the flows related to the AR, the inlet streams are controlled by mass flow regulators, as well with the Helium for the LS. At the outlet, after the cyclone, there exists a cooling and filtering step, followed by a pump and the final measurement tools: a volumetric flowmeter, a rotameter and a Non Dispersive Infrared Analyzer (NDIR), permitting online composition measurements.

The water content is only evaluated between the gasifying and reforming step. This is done by weighting the condensed water following gas cleaning process, right after the cooling procedure.

The tars are measured via Solid Phase Adsorption (SPA), from a sample collected up and another downstream, to analyze the tar destruction. This is done by inserting a syringe with a needle in orifices at the locations mentioned above and sucking a sample out.

This way, flow stream values and volumetric concentrations are measured.

Relatively to the data, it is important to present some aspects that might have had some influence on the data quality. They are mainly related to material limitations as well as a lack of operating personnel during the first experimental campaign.

Indeed, only one person performed the experiments. One consequence is in the accuracy of the controlling in pressure difference between the reactors while retiring manually wet gas samples for the SPA analyzes. If the pressure difference increases, the possibility of Nitrogen leaking from the AR to the FR increases.

### 3.3. Operational conditions and data used

Using the CLR system described before, different catalysts and oxygen concentrations in the AR were tested, in order to assess which ones are more suited for tar reforming. In the ambit of this work, two raw data sets were used, being the characteristics represented in table 5:

Table 5 - System conditions from the used raw data

| Bed material constitution |                     |             |                     |                        |  |
|---------------------------|---------------------|-------------|---------------------|------------------------|--|
| Catalyst                  | [%] <sub>mass</sub> | Inert       | [%] <sub>mass</sub> | Temperature(s)<br>[°C] | AR O <sub>2</sub><br>concentration(s)<br>[%] <sub>volume</sub> |
| Ilmenite                  | 60                  | Silica-sand | 40                  | 700,750 and<br>800     | 1  |
| Manganese                 | 23                  | Silica-sand | 77                  | 800                    | 1,01 and 2,18  |

From the SPA, different tar groups are measured. As for this model a simplified approach for the tars is considered, it was decided to use naphthalene as a representative compound. The explanation relies in the fact that the average molecular weight of all tars considers is near to 128 g/mol, which corresponds to the molecular weight of naphthalene.

Because naphthalene was chosen in this work as a representative compound for the tars, kinetic data taken from literature was used as a first approach in the attempt in modeling the tar behavior in the system. This data is shown in table 6:

Table 6 - Power law data for naphthalene (9)

| Power law data for naphthalene   |                      |
|----------------------------------|----------------------|
| Element                          | Reaction order       |
| Hydrocarbon (Tar)                | 1,6                  |
| Hydrogen                         | -0,5                 |
| Steam                            | 0                    |
| $k [m^{0,3} kmol^{-0,1} s^{-1}]$ | $3.4 \times 10^{14}$ |

## 4. Methodology

As first approach for this master thesis, a literature review was made. A big emphasis was given on reading articles related specifically to the CLR system in Chalmers (8) and its integration possibilities (5). So, an understanding of the concept and functioning of the system was accomplished and also a broader view related to other tar eliminating methods, in particular its advantages and disadvantages.

To process and analyze the complete data set, a MatLab file (Appendix II) was implemented in order to apply the balance to all measurements points closest to steady-state conditions. It was admitted that the system was in steady-state when reactor temperatures and FR in and out concentrations showed to be stabilized. Although total stationarity was highly improbable, these and further assumptions had to be made in order to make the model elaboration possible. Nevertheless, these are valid given the kind of measurements made.

Once access to the CLR data was given, the initial approach consisted in applying a system molar balance for the main existing elements (Carbon, Hydrogen, Oxygen and Nitrogen) in order to calculate missing stream flow values. This was necessary to fully characterize the system and, in future steps, permit Aspen Plus implementation. The balance was elaborated knowing in advance how and what kind of data was measured. Relevant comments associated with the measurements are mentioned with its correspondent nomenclature, used in the balances. Finally, an energy assessment was made, in order to analyze how well the elaborated model fits the experimental results energetically.

All values are obtained normalized to 25°C. Using the ideal gas molar volume ( $V_m$ ) of 22,4 l/mole, this allows easy conversion between volumetric flow in molar flows and vice-versa.

### 4.1. Variables overview

The present section aims at summarizing the different variables (flows, concentrations, etc.) used to achieve the system molar balance. These are all shown in the following table, Table 7.

Table 7 - Variable overview

| Variable                 | Description                    |
|--------------------------|--------------------------------|
| <b>FR</b>                |                                |
| $[X]_{FRin}$             | Dry compound concentration in  |
| $[X]_{FRout}$            | Dry compound concentration out |
| $g_{tarsin}$             | Tar concentration in           |
| $g_{tarsout}$            | Tar concentration out          |
| $w_{in}$                 | Water concentration in         |
| $\dot{n}_{FRout}^{H_2O}$ | Water molar flow out           |
| $\dot{n}_{FRin}^{dry}$   | Dry gas molar flow in          |
| $\dot{n}_{FRout}^{dry}$  | Dry gas molar flow out         |
| <b>AR</b>                |                                |
| $[X]_{ARout}$            | Dry compound concentration out |
| $\dot{n}_{ARout}$        | Gas molar flow out             |
| $\dot{n}_{ARin}^{O_2}$   | Oxygen molar flow in           |
| $\dot{n}_{ARin}^{N_2}$   | Nitrogen molar flow in         |

## 4.2. Molar balance calculations

All the values measured had to receive some adjustments, which are explained individually in the next topics. Also the system variables, the known and unknowns, are presented.

For a better understanding is presented a scheme with all components involved and their theoretical inlet/outlet system location:

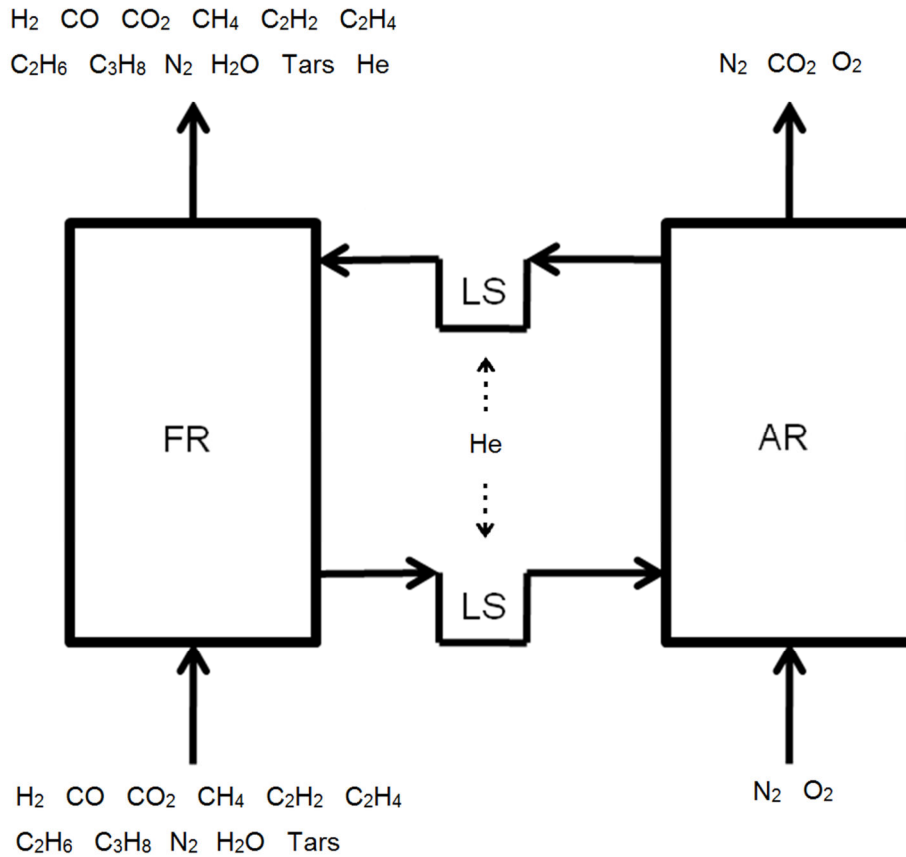


Figure 11 - Molar balance system streams overview

FR in and out concentrations ( $[CO]_{FR}$ ,  $[CO_2]_{FR}$ ,  $[CH_4]_{FR}$ , ...)

The volumetric concentrations of the non-condensable gases were measured with the GC. From the obtained values, it is expected to have  $O_2$  at 0%, as downstream from the gasifier and from the reforming system all oxygen should have been consumed. Due to air leakage in the tubes leading to the GC, the concentration values have to be corrected. Two equations are presented to show the correction made. A general compound's concentration is represented by the letter  $X_i$  and 10 compounds exist:  $H_2$ ,  $CO$ ,  $CO_2$ ,  $CH_4$ ,  $C_2H_2$ ,  $C_2H_4$ ,  $C_2H_6$ ,  $C_3H_8$ ,  $N_2$  and  $O_2$ . Note that  $N_2$  corresponds to  $i=9$  and  $O_2$  to  $i=10$ . While  $O_2$  is set to zero, to  $N_2$  is deduced the nitrogen presented in the air. Assuming an  $N_2/O_2$  ratio of 79/21, equation 18 gives the corrected  $N_2$  concentration:

$$[N_2]^{corrected} = \frac{[N_2] - [O_2] \cdot 21/79}{[N_2] - [O_2] \cdot 21/79 + \sum_{i=1}^{i=8} [X_i]} \cdot \sum_{i=1}^{i=10} [X_i]$$

Equation 18 -  $N_2$  correction

More generally, for a compound  $X_i$ :

$$[X_i]^{corrected} = \frac{[X_i]}{[N_2] - [O_2] \cdot 21/79 + \sum_{i=1}^{i=8} [X_i]} \cdot \sum_{i=1}^{i=10} [X_i]$$

Equation 19 - Element (Xi) correction

Contrarily to what is observed, the sum of all individual concentrations should theoretically be 100%. Calibration was made in order to measure specific gases, known to be the main constituents both from the raw and reformed gas. Relatively to the raw gas, the sum is rather near to the theoretical value, reaching values between 97% and 99%. Thus, a normalization is applied to bring the sum to 100%. This is only done after the air leakage correction mentioned before. Correction reads:

$$[X_i]^{normalized} = \frac{[X_i]}{\sum_{i=1}^{i=10} [X_i]} \cdot 100$$

Equation 20- Element (Xi) normalization

### Helium assumption

Analyzing the outlet concentrations, the sum of the concentrations of the exhaust ranges values between 70% and 80%. In chapter 3, it is mentioned that the LS are fluidized with Helium, which has to leave the system either through the AR or the FR. Unfortunately; no Helium concentration measurements were made. This problem is overcome by assuming that the gap between the sum and the supposed value of 100% is constituted by helium. The helium concentration reads:

$$[He]_{FR_{out}} = 100 - \sum_{i=1}^{i=10} [X_i]^{corrected}$$

Equation 21 - Helium concentration

As no further information about helium flows exist, this is viewed as the best way to incorporate the added inert gas in the calculations.

### Tar concentrations in and out of FR ( $g_{tars_{in}}$ resp. $g_{tars_{out}}$ )

Some level of uncertainty is associated with the tar concentrations as these were extracted manually. The tar concentrations are presented in  $g_{tar}/L_{dry\ gas}$ .

### H<sub>2</sub>O concentration in FR ( $w_{in}$ )

Similarly to the tars, the water concentration shows some uncertainty. As explained in chapter 3, it is measured by weighting both iso-propanol and water together and deriving how much water gathered during a specific amount of time. The unit is  $g_{water}/L_{dry\ gas}$ .

Dry gas flow out of FR ( $\dot{n}_{FRout}^{dry}$ )

Only the outlet flow is measured, because the inlet flow is at high temperature, making it unfeasible to lead the gases in. The flow control is made by a pump downstream from the FR that sucks the gas out. It is measured in units of L/min.

N<sub>2</sub> and O<sub>2</sub> flows in AR ( $\dot{n}_{ARin}^{N_2}$  resp.  $\dot{n}_{ARin}^{O_2}$ )

Nitrogen and air – thus oxygen - are measured with a flow meter, so their values have a low error, only associated related to equipment sensibility. Both are obtained with units of l/min.

CO<sub>2</sub> and O<sub>2</sub> concentrations out of AR ( $[CO_2]_{ARout}$ ,  $[O_2]_{ARout}$ )

Despite 4 gases leave the AR, only CO<sub>2</sub> and O<sub>2</sub> are measured, the two others being N<sub>2</sub> and He. The helium flow that leaves the AR is calculated via the previously mentioned assumption. So, the nitrogen concentration out of the AR can be deduced. These concentrations might also have a minor error associated, as the measured values lie near to the equipment's detection limit.

The unknowns of the balance are:

- $\dot{n}_{FRin}^{dry}$  – Dry inlet flow in the FR;
- $\dot{n}_{FRout}^{H_2O}$  – Water flow out of the FR;
- $\dot{n}_{ARout}$  – Total gas flow out of the AR;
- $[N_2]_{ARout}$  – Nitrogen concentration out of the AR.

Having 4 equations and 4 unknowns, the equation system is well-defined.

### 4.3. Molar balance

The elaborated system balance equations are presented below.

#### Carbon balance

$$\begin{aligned} & \dot{n}_{FRin}^{dry} \left[ \frac{[CO]_{FRin} + [CO_2]_{FRin} + [CH_4]_{FRin} + 2 \cdot [C_2H_2]_{FRin} + 2 \cdot [C_2H_4]_{FRin} + 2 \cdot [C_2H_6]_{FRin} + 3 \cdot [C_3H_8]_{FRin}}{100} \right] + \dot{n}_{FRin}^{dry} \cdot 10 \cdot g_{tarsin} \cdot \frac{V_m}{M_{tars}} \\ &= \dot{n}_{FRout}^{dry} \left[ \frac{[CO]_{FRout} + [CO_2]_{FRout} + [CH_4]_{FRout} + 2 \cdot [C_2H_2]_{FRout} + 2 \cdot [C_2H_4]_{FRout} + 2 \cdot [C_2H_6]_{FRout} + 3 \cdot [C_3H_8]_{FRout}}{100} \right] \\ &+ \dot{n}_{FRout}^{dry} \cdot 10 \cdot g_{tarsout} \cdot \frac{V_m}{M_{tars}} + \dot{n}_{ARout} \cdot \left[ \frac{[CO_2]_{ARout}}{100} \right] \end{aligned}$$

#### Equation 22- Carbon balance

#### Hydrogen balance

$$\begin{aligned} & \dot{n}_{FRin}^{dry} \left[ \frac{2 \cdot [H_2]_{FRin} + 4 \cdot [CH_4]_{FRin} + 2 \cdot [C_2H_2]_{FRin} + 4 \cdot [C_2H_4]_{FRin} + 6 \cdot [C_2H_6]_{FRin} + 8 \cdot [C_3H_8]_{FRin}}{100} \right] \\ &+ \dot{n}_{FRin}^{dry} \cdot 8 \cdot g_{tarsin} \cdot \frac{V_m}{M_{tars}} + \dot{n}_{FRin}^{dry} \cdot 2 \cdot w_{in} \cdot \frac{V_m}{M_{H_2O}} \\ &= \dot{n}_{FRout}^{dry} \left[ \frac{2 \cdot [H_2]_{FRout} + 4 \cdot [CH_4]_{FRout} + 2 \cdot [C_2H_2]_{FRout} + 4 \cdot [C_2H_4]_{FRout} + 6 \cdot [C_2H_6]_{FRout} + 8 \cdot [C_3H_8]_{FRout}}{100} \right] + \dot{n}_{FRout}^{dry} \cdot 8 \cdot g_{tarsout} \cdot \frac{V_m}{M_{tars}} \\ &+ \dot{n}_{FRout}^{H_2O} \cdot 2 \end{aligned}$$

#### Equation 23 - Hydrogen balance

#### Oxygen balance

$$\begin{aligned} & \dot{n}_{FRin}^{dry} \left[ \frac{2 \cdot [H_2]_{FRin} + 4 \cdot [CH_4]_{FRin}}{100} \right] + 2 \cdot \dot{n}_{ARin}^{O_2} + \dot{n}_{FRin}^{dry} \cdot w_{in} \cdot \frac{V_m}{M_{H_2O}} \\ &= \dot{n}_{FRout}^{dry} \left[ \frac{2 \cdot [H_2]_{FRout} + 4 \cdot [CH_4]_{FRout}}{100} \right] + \dot{n}_{FRout}^{H_2O} + \dot{n}_{ARout} \cdot \left[ \frac{2 \cdot [CO_2]_{ARout} + [O_2]_{ARout}}{100} \right] \end{aligned}$$

#### Equation 24 - Oxygen balance

## Nitrogen balance

$$\dot{n}_{ARin}^{N_2} + \dot{n}_{FRin}^{dry} \cdot \left[ \frac{[N_2]_{FRin}}{100} \right] = \dot{n}_{ARout} \cdot \left[ \frac{[N_2]_{ARout}}{100} \right] + \dot{n}_{FRout}^{dry} \cdot \left[ \frac{[N_2]_{FRout}}{100} \right]$$

### Equation 25 - Nitrogen balance

By analyzing the nitrogen balance it is visible that contrarily to the other balances, this one is not linear, as 2 unknowns are multiplying by each other:  $\dot{n}_{ARout}$  and  $([N_2])_{ARout}$ . Both variables can also be expressed in a simpler way using one variable:

$$\dot{n}_{ARout}^{N_2 f(balance)} = \dot{n}_{ARout} \cdot \left[ \frac{[N_2]_{ARout}}{100} \right]$$

### Equation 26 - Nitrogen out of AR, function of the balance

But, as the value related with the concentrations, is only present in equation 20, the system is solvable using only 3 unknowns ( $\dot{n}_{FRin}^{dry}$ ,  $\dot{n}_{FRout}^{H_2O}$  and  $\dot{n}_{ARout}$ ) and 3 equations (Carbon, Hydrogen and Oxygen). The remaining equation can be used once the 3 equation system is solved. Also, to verify if the nitrogen balance is near to be closed or not a residue sigma ( $\sigma$ ) is introduced. Comparing the molar flow of nitrogen leaving the system according to the balance with the flow taking into account the helium flow— ideally equal – it is possible to evaluate how near to be closed the  $N_2$  balance is.

Because the total inlet flow of helium is known and in conformity with the assumption made related to the FR outlet flow and the helium concentration, the following equation can be written to assess the flow of nitrogen the AR outlet:

$$\dot{n}_{ARout}^{N_2 f(He)} = \dot{n}_{ARout} \left( 1 - \frac{[CO_2]_{ARout} + [O_2]_{ARout}}{100} \right) - \left( \dot{n}_{Hein} - \dot{n}_{FRout}^{dry} \frac{[He]_{FRout}}{100} \right)$$

### Equation 27 - Nitrogen out of AR, function of the Helium balance

The residue calculation is given as:

$$\sigma = \frac{\dot{n}_{ARout}^{N_2 f(balance)} - \dot{n}_{ARout}^{N_2 f(He)}}{\dot{n}_{ARout}^{N_2 f(balance)}} \times 100$$

### Equation 28 - Nitrogen balance residue sigma in (%)

Given the balance nature, experimental data with elevated uncertainty, it is highly improbable that the residue reaches zero. Therefore, only a minimization criterion is applied.

In order to assess the AR flow variation from the inlet (taking into account the helium that enters the AR according to the assumption made) to the outlet more easily, the following expression is used:

$$\Delta \dot{n}_{AR} = \frac{\dot{n}_{ARout} - \dot{n}_{ARin(with\ Helium)}}{\dot{n}_{ARin}} \times 100$$

Equation 29 - AR flow variation in (%)

Also, to evaluate how the FR nitrogen flow changes, the expression above is used.

$$\Delta \dot{n}_{FR}^{N_2} = \frac{\dot{n}_{FRout}^{N_2} - \dot{n}_{FRin}^{N_2}}{\dot{n}_{FRin}^{N_2}} \times 100$$

Equation 30 - N2 FR flow variation in (%)

## 4.4. MatLab implementation

Once the equations were elaborated they were implemented in MatLab (Appendix II). Fig.12 shows a simple algorithm of the written program.



Figure 12 - MatLab scheme

The program inputs were read from an Excel file (Appendix III). As the inlet and outlet dry gases concentrations were not measured simultaneously, average input gas concentrations are calculated.

All possible combinations for outlet AR and FR concentrations are used to calculate the 3 system unknowns. The term “writes down realistic results” consists in only considering the positive stream flows. As the balance is merely a mathematical operation, it can happen that the solving gives negative stream flow values, which is not realistic and so these results are excluded.

The final step consists in saving the results in an Excel file (Appendix IV), for a facilitated result analysis.

## 4.5. Aspen Plus

The final step of the work consisted in building the Aspen Plus Model. The functionalities used are described in chapter 2.

Using the calculated streams and having the system totally defined, a mass balance only focused on the FR is calculated, in order to obtain the data necessary for further Aspen input and comparison. From all the calculated balances for each different combination, a representative case for each system condition is selected. The criteria for selecting the representative data was:

- Nitrogen entering the FR is equal or lower than nitrogen leaving the FR
- AR outlet stream is lower than the AR inlet stream
- Residue from the nitrogen balance has to be minimum

Indeed, as described in chapter 3, the AR pressure is slightly higher than the one from the FR. This makes it possible that, additionally to the catalyst transfer, a nitrogen leakage can even occur. Therefore, only balances where the N<sub>2</sub> content is higher or at minimum equal in the outlet relatively to the inlet are considered. Because the nitrogen balance should also be respected, the residue from its balance must be minimal.

In reality, the CLR is constituted by 2 reactors, but in the modeling only a coarse model with one reactor representing the FR is used. This relies in the fact that there is still to little detail on the processes happening inside the reactor. In particular, relevant detail on catalyst oxidation/reduction and tar reforming kinetics are not available. Thus, it makes fine modeling rather difficult and therefore a simpler model was considered.

Left with only one reactor, it is necessary to match the gas quantities that enter the experimental reactor and the model reactor so that in a more advanced step, it is possible to compare software and the experimental data. The input for the Aspen model is given from the molar balance, so the purpose is to fit the simulated results with the output derived from the experimental data.

Table 8 shows the principal gas streams that enter and leave the FR with their corresponding calculation formula and using all the measured data and molar balance results.

Table 8 - Flows calculation formulas

| Flow ( <i>mole/min</i> )        | FR Inlet  | FR Outlet                                    |
|---------------------------------|---|--|
| $\dot{n}_{H_2}$                 | $[H_2]_{in} \cdot \dot{n}_{FRin}^{dry}$                                   | $[H_2]_{out} \cdot \dot{n}_{FRout}^{dry}$    |
| $\dot{n}_{CO}$                  | $[CO]_{in} \cdot \dot{n}_{FRin}^{dry}$                                    | $[CO]_{out} \cdot \dot{n}_{FRout}^{dry}$     |
| $\dot{n}_{CO_2}$                | $[CO_2]_{in} \cdot \dot{n}_{FRin}^{dry}$                                  | $[CO_2]_{out} \cdot \dot{n}_{FRout}^{dry}$   |
| $\dot{n}_{CH_4}$                | $[CH_4]_{in} \cdot \dot{n}_{FRin}^{dry}$                                  | $[CH_4]_{out} \cdot \dot{n}_{FRout}^{dry}$   |
| $\dot{n}_{C_2H_2}$              | $[C_2H_2]_{in} \cdot \dot{n}_{FRin}^{dry}$                                | $[C_2H_2]_{out} \cdot \dot{n}_{FRout}^{dry}$ |
| $\dot{n}_{C_2H_4}$              | $[C_2H_4]_{in} \cdot \dot{n}_{FRin}^{dry}$                                | $[C_2H_4]_{out} \cdot \dot{n}_{FRout}^{dry}$ |
| $\dot{n}_{C_2H_6}$              | $[C_2H_6]_{in} \cdot \dot{n}_{FRin}^{dry}$                                | $[C_2H_6]_{out} \cdot \dot{n}_{FRout}^{dry}$ |
| $\dot{n}_{C_3H_8}$              | $[C_3H_8]_{in} \cdot \dot{n}_{FRin}^{dry}$                                | $[C_3H_8]_{out} \cdot \dot{n}_{FRout}^{dry}$ |
| $\dot{n}_{N_2}$                 | $[N_2]_{in} \cdot \dot{n}_{FRin}^{dry}$                                   | $[N_2]_{out} \cdot \dot{n}_{FRout}^{dry}$    |
| $\dot{n}_{O_2 \text{ from AR}}$ | $\dot{n}_{ARin}^{O_2} - (\dot{n}_{ARout}^{O_2} + \dot{n}_{ARout}^{CO_2})$ | -  |
| $\dot{n}_{He}$                  | -   | $[He]_{out} \cdot \dot{n}_{FRout}^{dry}$     |
| $\dot{n}_{tars}$                | $\dot{n}_{FRin}^{dry} \cdot g_{tarsin}$                                   | $\dot{n}_{FRout}^{dry} \cdot g_{tarsout}$    |
| $\dot{n}_{H_2O}$                | $\dot{n}_{FRin}^{dry} \cdot w_{in}$                                       | $\dot{n}_{FRout}^{H_2O}$                     |

The calculated inlet values were used as an input for the Aspen Plus flow sheet (Appendix VI). In reality, the helium flow  $\dot{n}_{He}$  enters the FR through the LS and the oxygen flow  $\dot{n}_{O_2 \text{ from AR}}$  with the catalyst through the SLS. As mentioned before, because only one reactor is used in this model, both of these flows are considered to be mixed with the raw gas from the beginning. Afterwards, applying tools included in the software used, the model outlet flow is adjusted in order to fit the FR outlet flows (see Table 8) in order to eventually achieve a model that can be representative of the CLC system.

A scheme showing the model is presented in the following figure:

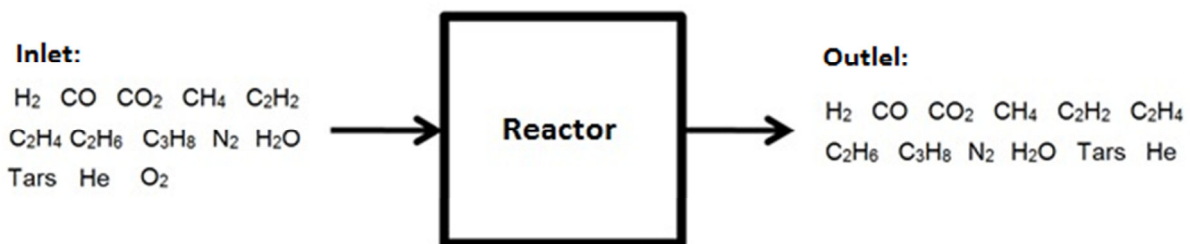


Figure 13 - In and outlet flow scheme in Aspen model

Two main approaches were used in this work: temperature approach and variation in the chemical constant.

### Temperature approach scheme for the reactor modeling

By changing a specific equilibrium reaction temperature for a specific reaction (e.g., tar reforming), different than the one from the reactor, it is possible to influence the composition of the gas at the outlet until they fit the experimental results. This is performed in the Equilibrium reactor and can be viewed as an iterative process. Figure 14 shows the scheme applied.

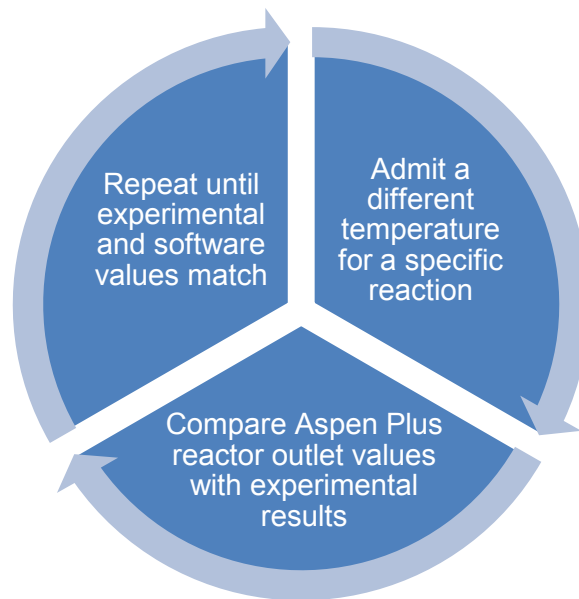


Figure 14 - Temperature approach scheme

### Variation in chemical constant

A different approach consists in performing an iterative process changing the pre-exponential constant ( $k$ ) in a “Arrhenius-type” equation and describing gas chemical reaction kinetics. As it is performed in the Plug flow reactor, all reactions and correspondent power-law values have to be specified. The objective is to find  $k$  values for each reaction yield similar molar flows of gas between the outlet streams obtained from the molar balances and the software results. A similar scheme to the temperature approach is considered by replacing the temperature admitted by an admitted value of  $k$  in the diagram. The reactor is also designed in a way that the gases have a similar residence time to the measured reactor residence time.

## 4.6. Energetic assessment

After calculating and comparing all the values, an energy study of the system is made. This is done in order to assess how the CLR behaves in energy terms. When going through the CLR, not only the tars are converted but also other gases containing a chemical energy ( $H_2$ ,  $CO$ ,  $CH_4$ ,  $C_2H_2$ ,  $C_2H_4$ ,  $C_2H_6$  and  $C_3H_8$ ) might be oxidized, causing some combusting heat value to be lost in the reformed gas stream. This goes against the initial purpose of increasing the heating value by adding the energy stored in the tars, which are catalytically converted into usable gases and so usable energy.

The energy assessment is performed by taking into account specific gases that are chemical energy carriers:  $H_2$ ,  $CO$ ,  $CH_4$ ,  $C_2H_2$ ,  $C_2H_4$ ,  $C_2H_6$  and  $C_3H_8$ . Their heating value and corresponding quantity up and down-stream enable the comparison between the chemical energy existing before and after the CLR. So, it is possible to assess how the chemical energy in the gas varies.

In order to do the energetic assessment, the logic in the next figure is used:

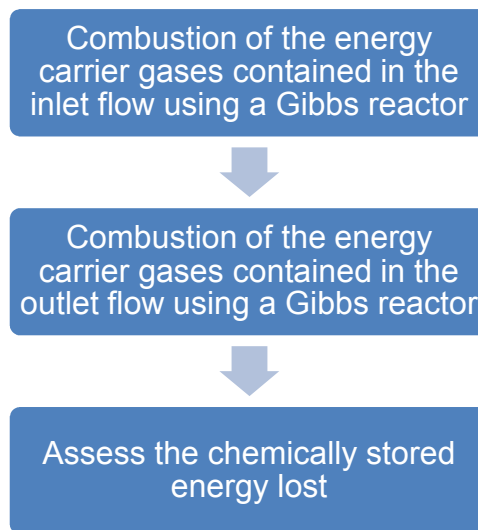


Figure 15 - Energy assessment scheme

This way it is possible to evaluate the quantity of chemically stored energy that is gained / lost. The assessment is done using equation 29 ... :

$$\Delta H_{CLR} = \frac{\Delta H_{outlet\ gases}^{298\ K} - \Delta H_{inlet\ gases}^{298\ K}}{\Delta H_{inlet\ gases}^{298\ K}} \times 100$$

Equation 31 - Combustion heat change between in and outlet gases in (%)

This procedure can be applied to both experimental and simulation results and therefore can as well give indications on how well the ASPEN modeled reactors describe the real one.

## 5. Results and discussion

### 5.1. Molar balance

All the possible combinations between the AR and the FR concentrations result in a long list of results for the molar balance, with Excel files reaching up to 10000 lines (Appendix IV), making it unrealizable to present all the results. Nevertheless, because most of the measurements, specially the AR out concentrations (Appendix III) which also are measured each second, repeat itself, the results can be summed up into a shorter but still representative list. Analyzing the same list and using the criteria mentioned before in section 4.5., the data for the Aspen Plus model is selected.

In the following tables, results for each experimental configuration are represented. In particular they include the AR total flow variation, the sigma criteria defined in equation 28 and the FR nitrogen flow variation.

#### 5.1.1. 60% Ilmenite / 40% Silica-sand and 1% oxygen in AR

The ilmenite data included 3 different oven temperatures: 700°C, 750°C and 800°C. The results for the corresponding molar balances are summarized in Table 9:

Table 9 - Molar balance results

| Results ID   | $\dot{n}_{FRin}^{dry}$ | $\dot{n}_{FRout}^{H_2O}$ | $\dot{n}_{ARin}$ | $\dot{n}_{ARout}$ | $\dot{n}_{ARout}^{N_2^{f(balance)}}$ | $\dot{n}_{ARout}^{N_2^{f(He)}}$ | $\dot{n}_{FRin}^{N_2}$ | $\dot{n}_{FRout}^{N_2}$ |
|--------------|------------------------|--------------------------|------------------|-------------------|--------------------------------------|---------------------------------|------------------------|-------------------------|
| [mole/min]   |                        |                          |                  |                   |                                      |                                 |                        |                         |
| <b>700°C</b> |                        |                          |                  |                   |                                      |                                 |                        |                         |
| T700-1       | 0,0727                 | 0,0789                   | 0,2559           | 0,0049            | 0,2338                               | -0,0201                         | 0,0156                 | 0,0163                  |
| T700-2       | 0,0709                 | 0,077                    | 0,2553           | 0,0483            | 0,2344                               | 0,0231                          | 0,0153                 | 0,0149                  |
| T700-3       | 0,0714                 | 0,0777                   | 0,2556           | 0,1435            | 0,2343                               | 0,1181                          | 0,0154                 | 0,0153                  |
| T700-4       | 0,0709                 | 0,0770                   | 0,2553           | 0,0473            | 0,2344                               | 0,0221                          | 0,0153                 | 0,0149                  |
| <b>750°C</b> |                        |                          |                  |                   |                                      |                                 |                        |                         |
| T750-1       | 0,0608                 | 0,0586                   | 0,2552           | 0,1414            | 0,2343                               | 0,1160                          | 0,0131                 | 0,0128                  |
| T750-2       | 0,063                  | 0,0615                   | 0,2563           | 0,2496            | 0,2344                               | 0,2239                          | 0,0138                 | 0,0133                  |
| T750-3       | 0,0636                 | 0,0615                   | 0,2563           | 0,2581            | 0,2344                               | 0,2323                          | 0,0138                 | 0,0133                  |
| T750-4       | 0,0603                 | 0,601                    | 0,2558           | 0,2636            | 0,2340                               | 0,2379                          | 0,0134                 | 0,0137                  |
| T750-5       | 0,0597                 | 0,0595                   | 0,2556           | 0,2415            | 0,2341                               | 0,2159                          | 0,0133                 | 0,0133                  |
| <b>800°C</b> |                        |                          |                  |                   |                                      |                                 |                        |                         |
| T800-1       | 0,0618                 | 0,0582                   | 0,2561           | 0,1381            | 0,2345                               | 0,1128                          | 0,0133                 | 0,0126                  |
| T800-2       | 0,0596                 | 0,0544                   | 0,2565           | 0,2336            | 0,2342                               | 0,2080                          | 0,0128                 | 0,0127                  |
| T800-3       | 0,585                  | 0,0531                   | 0,2562           | 0,2736            | 0,2342                               | 0,2482                          | 0,0126                 | 0,0126                  |
| T800-4       | 0,0565                 | 0,0512                   | 0,2559           | 0,2480            | 0,2328                               | 0,2225                          | 0,0121                 | 0,0149                  |

The next table contains the flow variations, expressed in relative terms, using equations 28, 29 and 30. The order is the same as in table 9, above.

Table 10 - Results variation

| Results ID   | $\Delta\dot{n}_{AR}$ | $\sigma$ | $\Delta\dot{n}_{FR}^{N_2}$ | Results ID   | $\Delta\dot{n}_{AR}$ | $\sigma$ | $\Delta\dot{n}_{FR}^{N_2}$ |
|--------------|----------------------|----------|----------------------------|--------------|----------------------|----------|----------------------------|
| [%]          |                      |          |                            |              |                      |          |                            |
| <b>700°C</b> |                      |          |                            | <b>800°C</b> |                      |          |                            |
| T700-1       | -98,1                | 108,6    | 4,6                        | T800-1       | -46,1                | 51,9     | -5,0                       |
| T700-2       | -81,1                | 90,1     | -2,5                       | T800-2       | -8,9                 | 11,2     | -0,9                       |
| T700-3       | -43,9                | 49,6     | -1,1                       | T800-3       | 6,8                  | -6,0     | 0,1                        |
| T700-4       | -81,5                | 90,6     | -2,5                       | T800-4       | -3,1                 | 4,4      | 23,0                       |
| <b>750°C</b> |                      |          |                            |              |                      |          |                            |
| T750-1       | -44,6                | 50,5     | -2,0                       |              |                      |          |                            |
| T750-2       | -2,6                 | 4,5      | -3,7                       |              |                      |          |                            |
| T750-3       | 0,7                  | 0,9      | -3,7                       |              |                      |          |                            |
| T750-4       | 3,1                  | -1,7     | 2,4                        |              |                      |          |                            |
| T750-5       | -5,5                 | 7,8      | 0,5                        |              |                      |          |                            |

Considering Tables 9 and 10, it is seen that the 700°C case gives odd results. There are extremely high differences between the inlet and the outlet of the AR. It is expected that some N<sub>2</sub> leakage occurs due to the slight pressure difference between reactors and also that the oxygen present in the AR is transported with the oxygen carrier/catalyst into the FR, however it is highly improbable that 98 or 44% of the AR inlet flow leaks into the FR. Knowing that the FR outlet dry flow is kept around 2 L/min and comparing all the FR inlet flows for each different temperature, is another reason for affirming that the AR flow differences cannot be so elevated. In consequence, the agreement between the differently calculated nitrogen flows is also low, translating into a high sigma value.

In the experimental procedure, the system was started without introducing raw gas in the FR. At initialization, only catalyst circulation with AR containing oxygen and nitrogen was occurring. Once the raw gas was introduced, ilmenite was already saturated with oxygen which could not be taken into account in the molar balance. Analyzing the O<sub>2</sub> concentrations during the 700°C experiment, it is visible that it has higher values than the other temperatures (e.g. 0,22% for 700°C compared to 0,02% for 800°C) and CO<sub>2</sub> concentrations with similar magnitudes (e.g. 0,21% compared to 700°C and 0,13 % for 800°C). This indicates that the variation in oxygen available to convert tars is a result of the start-up procedure. Therefore, the molar balance applied is not valid for the starting temperature, once an unknown quantity of oxygen is present in the system. Moreover, during the early phase of operation, which coincides with the 700°C case, the fresh Ilmenite material is gradually activated and thus the system was not stable (8).

On the contrary, for the cases at higher temperature, the concentrations from the gas leaving the AR have now lower O<sub>2</sub> concentrations, indicating that the oxygen entering is being transported by the catalyst into the FR, and also that catalyst is reaching full activation.

Regarding the imposed conditions for the selection of the best data, the data possible to be representative of each temperature is presented in the next table:

Table 11 - Candidate data for Aspen Plus

| Results ID   | $\Delta\dot{n}_{AR}$ | $\sigma$ | $\Delta\dot{n}_{FR}^{N_2}$ | Results ID   | $\Delta\dot{n}_{AR}$ | $\sigma$ | $\Delta\dot{n}_{FR}^{N_2}$ |
|--------------|----------------------|----------|----------------------------|--------------|----------------------|----------|----------------------------|
| [%]          |                      |          |                            |              |                      |          |                            |
| <b>750°C</b> |                      |          |                            | <b>800°C</b> |                      |          |                            |
| T750-2       | -2,6                 | 4,5      | -3,7                       | T800-2       | -8,9                 | 11,2     | -0,9                       |
| T750-3       | 0,7                  | 0,9      | -3,7                       | T800-3       | 6,8                  | -6,0     | 0,1                        |
| T750-4       | 3,1                  | -1,7     | 2,4                        | T800-4       | -3,1                 | 4,4      | 23,0                       |
| T750-5       | -5,5                 | 7,8      | 0,5                        | -            | -                    | -        | -                          |

Observing Table 11, it would of no importance which data should be used and knowing the errors associated with the experiments and comparing each flow result is a valid affirmation. Nevertheless, only to be as coherent as possible with the selection criteria, for the 750°C case were chosen the values T750-5, while for 800°C, the T800-4 were used. Indeed, the sigma is as low as possible, the nitrogen AR flow difference has a negative value, which admits that gas leaks occur from the AR to the FR and not otherwise, and the same for the nitrogen increase in the FR, where the nitrogen flow is supposed to stay equal or increase.

It is clear that the sigma and AR flow change have extremely high values although the nitrogen flow variation is within a realistic range. In the data analysis section (6.2.1) it is shown how sensitive the AR outlet flow is with respect to the AR outlet concentrations while the FR flows remain with stable values.

### 5.1.2. 23% Manganese / 77% Silica-sand at 800°C

For the manganese experiment 2 different volumetric oxygen concentrations were used, 1,01% and 2,18% in the AR. The results read:

Table 12 - Molar balance results

| Results ID                 | $\dot{n}_{FRin}^{dry}$ | $\dot{n}_{FRout}^{H_2O}$ | $\dot{n}_{ARin}$ | $\dot{n}_{ARout}$ | $\dot{n}_{ARout}^{N_2^{f(balance)}}$ | $\dot{n}_{ARout}^{N_2^{f(He)}}$ | $\dot{n}_{FRin}^{N_2}$ | $\dot{n}_{FRout}^{N_2}$ |
|----------------------------|------------------------|--------------------------|------------------|-------------------|--------------------------------------|---------------------------------|------------------------|-------------------------|
| [mole/min]                 |                        |                          |                  |                   |                                      |                                 |                        |                         |
| <b>1,01% O<sub>2</sub></b> |                        |                          |                  |                   |                                      |                                 |                        |                         |
| T1-1                       | 0,08467                | 0,08085                  | 0,26381          | 11,78199          | 0,21799                              | 11,73835                        | 0,00966                | 0,01666                 |
| T1-2                       | 0,08894                | 0,08783                  | 0,26381          | 7,14472           | 0,21848                              | 7,10097                         | 0,01014                | 0,01666                 |
| T1-3                       | 0,08551                | 0,08472                  | 0,26160          | 6,92976           | 0,22261                              | 6,88633                         | 0,00975                | 0,01214                 |
| <b>2,18% O<sub>2</sub></b> |                        |                          |                  |                   |                                      |                                 |                        |                         |
| T2-1                       | 0,10892                | 0,12208                  | 0,26144          | 8,99657           | 0,21245                              | 8,93655                         | 0,01242                | 0,01158                 |
| T2-2                       | 0,10188                | 0,11756                  | 0,25934          | 3,66798           | 0,21136                              | 3,61294                         | 0,01162                | 0,01187                 |
| T2-3                       | 0,10408                | 0,11939                  | 0,25967          | 3,80155           | 0,21236                              | 3,74570                         | 0,01187                | 0,01112                 |

For a better understanding, the results are presented in relative terms in the Table 13:

Table 13 - Results variation

| Results ID                 | $\Delta\dot{n}_{AR}$ | $\sigma$ | $\Delta\dot{n}_{FR}^{N_2}$ | Results ID                 | $\Delta\dot{n}_{AR}$ | $\sigma$ | $\Delta\dot{n}_{FR}^{N_2}$ |
|----------------------------|----------------------|----------|----------------------------|----------------------------|----------------------|----------|----------------------------|
| [%]                        |                      |          |                            |                            |                      |          |                            |
| <b>1,01% O<sub>2</sub></b> |                      |          |                            | <b>2,18% O<sub>2</sub></b> |                      |          |                            |
| T1-1                       | 4366,1               | -5284,8  | 72,6                       | T2-1                       | 3341,2               | -4106,4  | -6,8                       |
| T1-2                       | 2608,3               | -3150,2  | 64,3                       | T2-2                       | 1314,4               | -1609,4  | 2,2                        |
| T1-3                       | 2549,0               | -2993,4  | 24,5                       | T2-3                       | 1364,0               | -1663,9  | -6,3                       |

Analyzing both data from Table 12 and 13, it is observed that the balance is hardly closed. The variance corresponding to the nitrogen flow in the FR is within acceptable leakage ranges but on the other hand both AR flow and sigma values are too high, which gives indications that there might be some errors in the measurement. Therefore, the manganese data was considered not suitable to implement in ASPEN.

## 5.2. Data analysis

Following the data selection presented in section 5.1, it was possible to know which data to use to proceed with the software implementation. In order to get a deeper knowledge of the results and how they can vary, since they depend on different concentrations with different orders of magnitude, a sensibility analysis is performed. The analysis will be performed by inspecting how changing each molar balance input (component concentration at the FR inlet, component concentration at the FR outlet tar concentrations, etc.) influences the final results. By using this procedure, it is assessed at what level errors and uncertainties in the measurements could induce changes in the results.

In total, there are 38 different analyses possible to be made, so 38 graphs only for 1 system condition. All the results are presented in an Appendix (Appendix V), while in this section, only some are mentioned.

The labels for all the graphics are shown in Fig.16:

- ◆ FR in dry
- FR out H2O
- ▲ AR out
- ✕ N2 out AR - balance

Figure 16 - Graph label

### 5.2.1. 60% Ilmenite / 40% Silica-sand and 1% oxygen in AR

For the ilmenite case, the sensibility analysis will be performed for the 800°C case, starting with results T800-4. Indeed, for the other temperatures the conclusions will be the same, because all values have the same order of magnitude.

The sensitivity analysis graphs are displayed in the following Figs. 17 to 26.

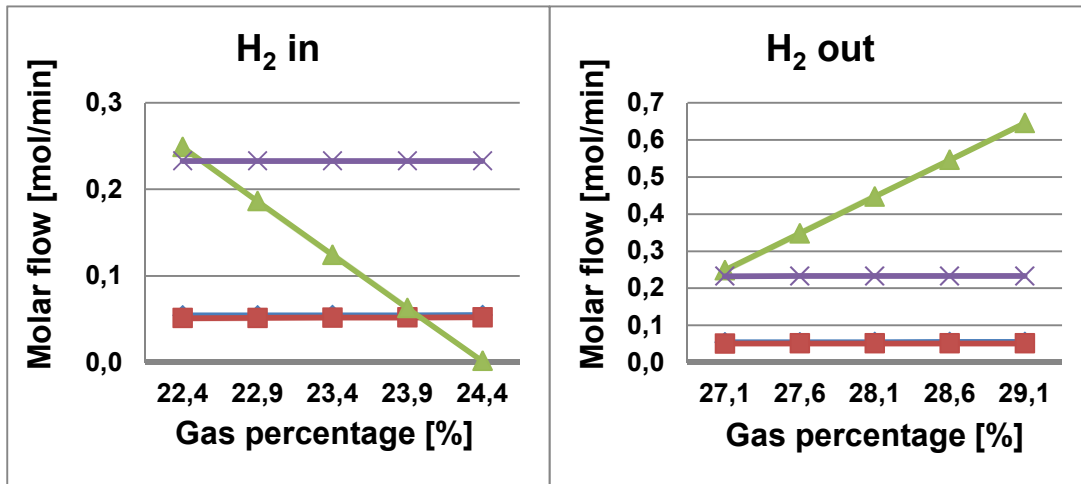


Figure 18 - Hydrogen FR in sensitivity analysis

Figure 17 - Hydrogen FR out sensitivity analysis

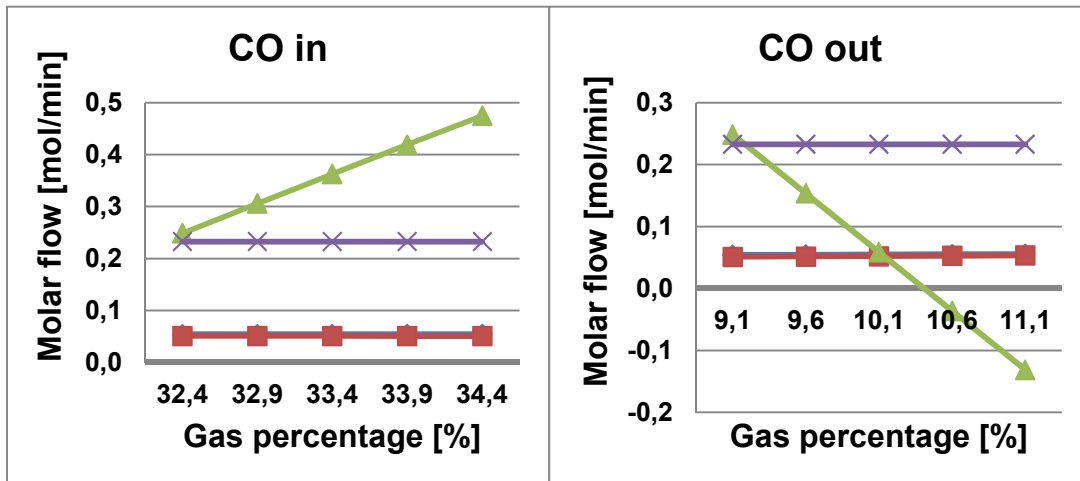


Figure 20 - Carbon Monoxide FR in sensitivity analysis

Figure 19 - Carbon Monoxide FR out sensitivity analysis

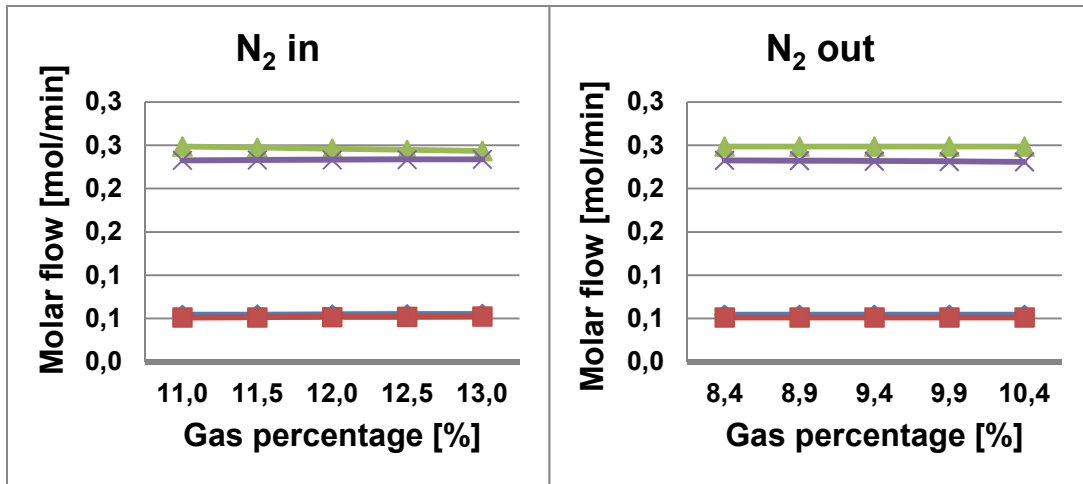


Figure 22 - Nitrogen FR in sensitivity analysis

Figure 21 - Nitrogen FR out sensitivity analysis

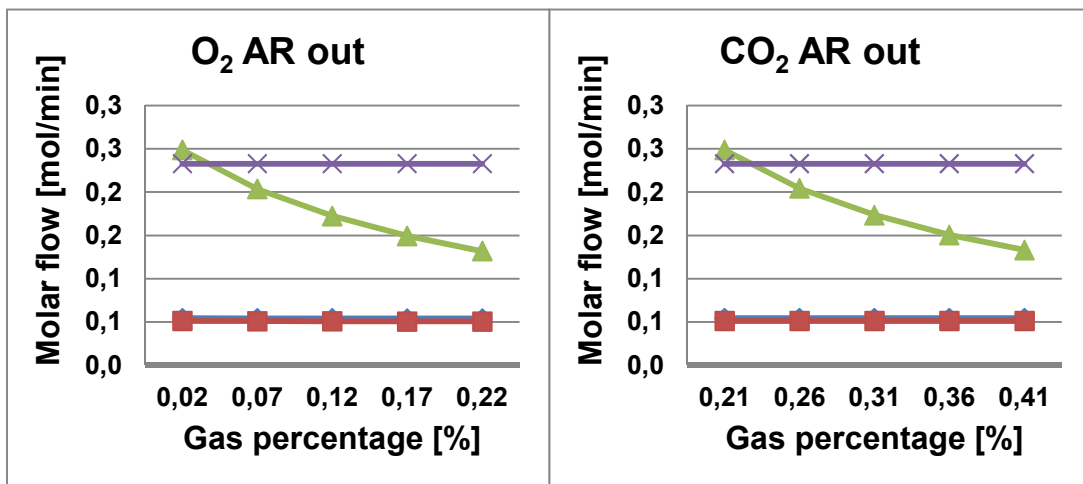


Figure 24 - Oxygen AR out sensitivity analysis

Figure 23 - Carbon Dioxide FR out sensitivity analysis

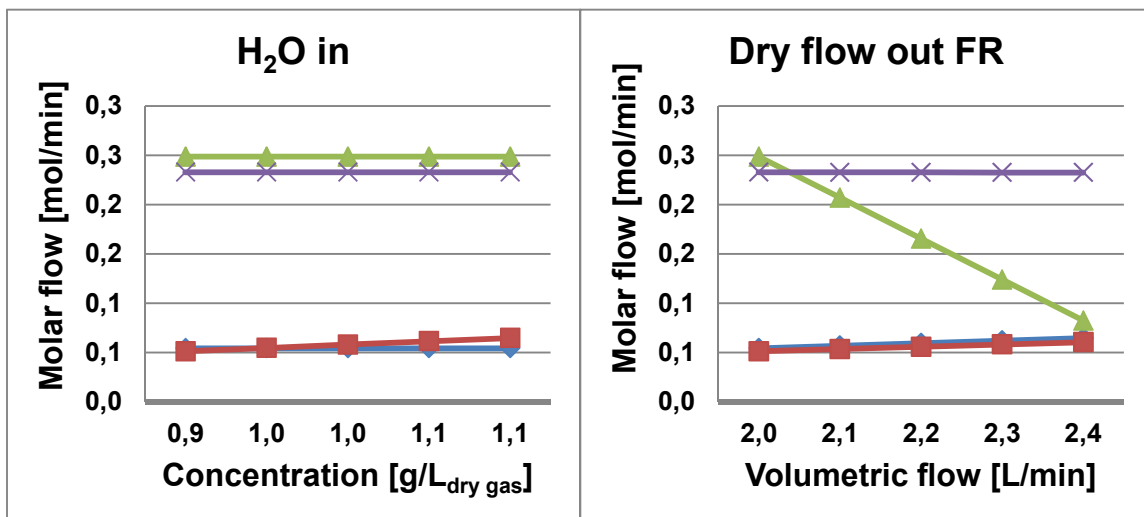


Figure 26 - Water FR in sensitivity analysis

Figure 25 - Dry flow FR out sensitivity analysis

It is seen from the figures above that the most sensitive result is the total AR outlet flow. This is easily explained by the fact that when solving the molar balance, the numeric coefficients associated ( $\text{CO}_2$  and  $\text{O}_2$  concentrations out of the AR) with this unknown are 1 or 2 orders of magnitude lower than the remaining ones. Therefore, a slight variation in the input values causes a higher change in this value. Nevertheless, this value is not a critical result for the Aspen Plus model, as only the FR is mainly being considered.

The important flows for the software implementation (FR inlet dry flow and FR outlet  $\text{H}_2\text{O}$  flow) are clearly more stable and have a low response to changes in the input values. There might be cases where e.g. the " $\text{H}_2\text{O}$ " in and the "Dry flow out FR" flows change but this is because they have a more direct relation with the input values. If these inputs increase it is obvious that the inlet flow and the water flow in increase as well because a balance is being applied.

1% is the error for the FR dry gases concentrations and for the other measurements they are difficult to define (e.g. tar concentration,  $\text{H}_2\text{O}$  concentration, etc) Also important to mention is that the AR out concentrations have a tendency to show rather high errors as the values measured with the NDIR were critically near the detection limit.

Even with the errors associated with the measurements, it is viable to use the results to improve the ASPEN model, once again, because the errors and changes that they might involve correspond to a low alteration upon the results needed for implementation.

### **5.2.2. 23% Manganese / 77% Silica-sand at 800°C**

For the manganese sensitivity analysis, the data related to 2.18 % case. The data is presented in the following graphs, Figs 27 to 36.

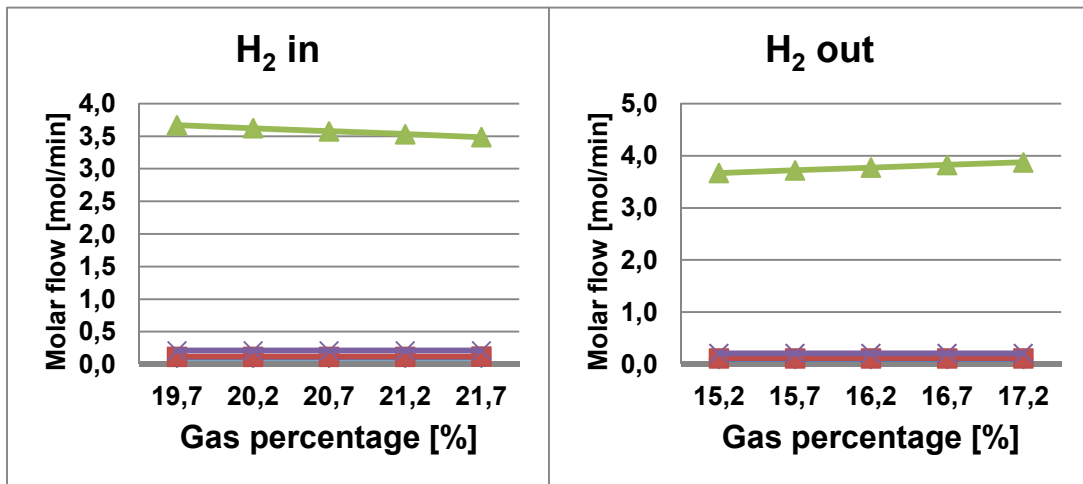


Figure 28 - Hydrogen FR in sensitivity analysis

Figure 27 - Hydrogen FR out sensitivity analysis

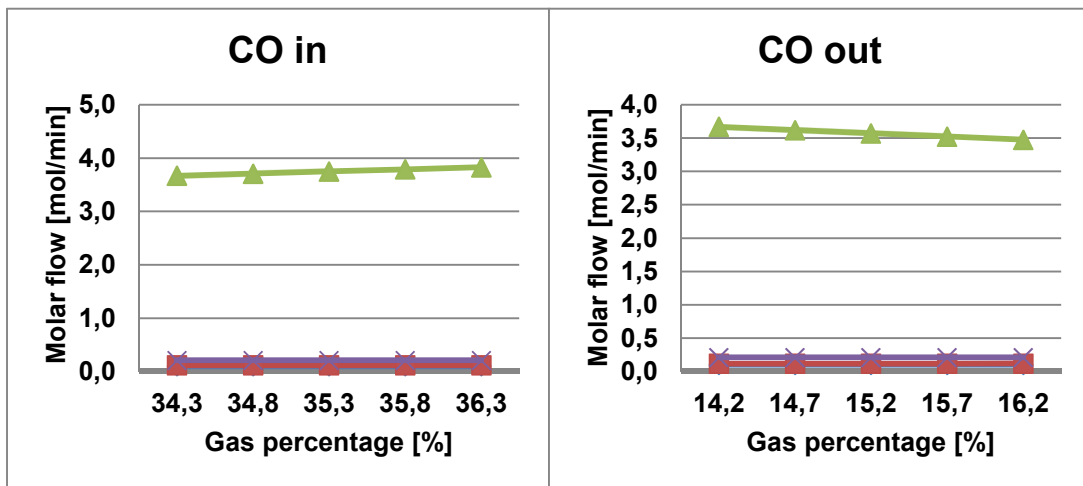


Figure 30 - Carbon Monoxide FR in sensitivity analysis

Figure 29 - Carbon Monoxide FR out sensitivity analysis

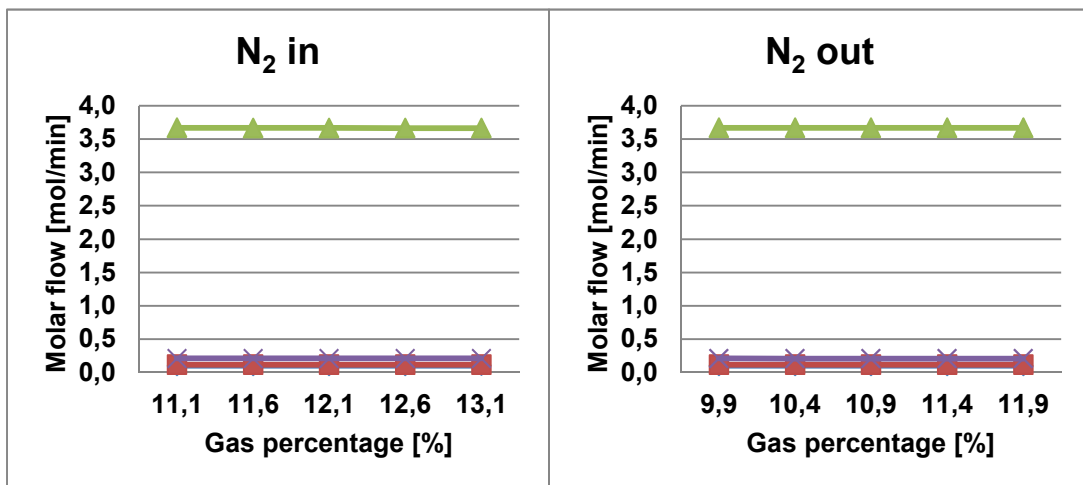


Figure 32 - Nitrogen FR in sensitivity analysis

Figure 31 - Nitrogen FR out sensitivity analysis

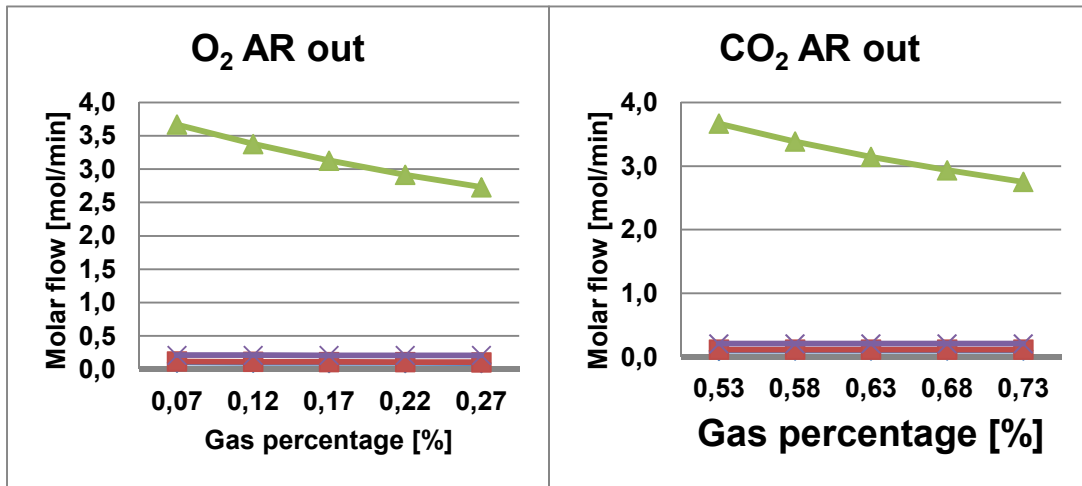


Figure 34 - Oxygen AR out sensitivity analysis

Figure 33 - Carbon Dioxide AR out sensitivity analysis

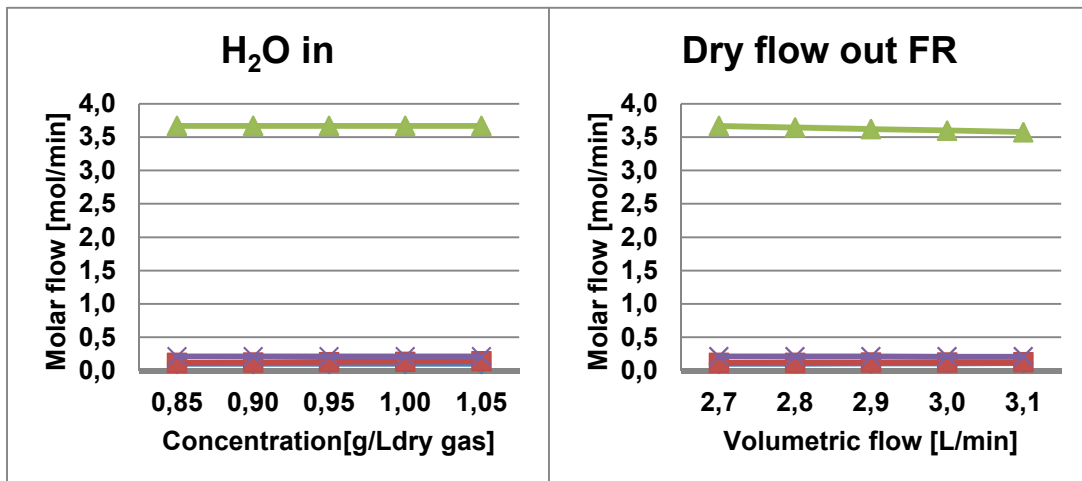


Figure 36 - Water FR in sensitivity analysis

Figure 35 - Dry flow FR out sensitivity analysis

Almost no influence is noticed in the flow values when changing FR in and outlet concentrations, contrary to the Ilmenite case. As in the molar balance, high and unrealistic results appear for the AR out flow value it is normal that small changes in the FR flows values have a low influence on the latter flow.

However, changes of the AR out concentrations have a considerable influence on the AR out flow.

Generally, changing the carbon containing elements concentration has always a notable influence on the total flow leaving the AR, as well as the oxygen flow entering in the AR. This happens, as explained before, because the latter unknown is associated to a very low numerical coefficient.

### 5.3. Aspen and balance comparison

In this section are displayed all the Aspen Plus results, including all the simplification mentioned before, with further comparison from the values obtained with the molar balance. It is important not to forget that the simulations consider a single reactor so, all the components that in the real system enter through different inlets (Helium derived from the LS and oxygen transported into the FR with the catalyst) are inserted in the simulation reactor through one single inlet.

It is important to mention that the only two equations were considered in the simulations: water-gas shift and steam tar reforming.

For the temperature approach and the plug flow reactor, the model optimization is done using the steam reforming reaction, by fitting the outlet model tar flow with the outlet tar flow obtained from the measurements.

The results are obtained using the reactors displayed in section 2.4.

#### 5.3.1. 60% Ilmenite, 40% Silica-sand and 1% oxygen in AR

First, a table with the variations that occurred in the experimental facility is. See Table 14 .

Table 14 - Component molar FR balance results

| Temperature                     | 750°C               |         |      | 800°C                     |         |      |
|---------------------------------|---------------------|---------|------|---------------------------|---------|------|
|                                 | Flows<br>[mole/min] | In      | Out  | $\Delta_{balance}$<br>[%] | In      | Out  |
| $\dot{n}_{H_2}$                 | 0,01363             | 0,02159 | 58   | 0,01247                   | 0,02420 | 94   |
| $\dot{n}_{CO}$                  | 0,01969             | 0,00935 | -52  | 0,01801                   | 0,00811 | -55  |
| $\dot{n}_{CO_2}$                | 0,00915             | 0,01981 | 117  | 0,00837                   | 0,02013 | 141  |
| $\dot{n}_{CH_4}$                | 0,00740             | 0,00753 | 2    | 0,00677                   | 0,00714 | 6    |
| $\dot{n}_{C_2H_2}$              | 0,00022             | 0,00003 | -88  | 0,00020                   | 0,00003 | -86  |
| $\dot{n}_{C_2H_4}$              | 0,00256             | 0,00245 | -4   | 0,00234                   | 0,00173 | -26  |
| $\dot{n}_{C_2H_6}$              | 0,00023             | 0,00024 | 3    | 0,00021                   | 0,00007 | -67  |
| $\dot{n}_{C_3H_8}$              | 0,00012             | 0,00000 | -100 | 0,00011                   | 0,00000 | -100 |
| $\dot{n}_{N_2}$                 | 0,00667             | 0,00667 | 0    | 0,00610                   | 0,00746 | 22   |
| $\dot{n}_{O_2 \text{ from AR}}$ | 0,00188             | 0,00000 | -100 | 0,00187                   | 0,00000 | -100 |
| $\dot{n}_{tars}$                | 0,00028             | 0,00026 | -8   | 0,00026                   | 0,00018 | -30  |
| $\dot{n}_{H_2O}$                | 0,06726             | 0,05952 | -11  | 0,06153                   | 0,05119 | -17  |
| $\dot{n}_{He}$                  | 0,02162             | 0,02162 | 0    | 0,02040                   | 0,02040 | 0    |

In the molar balance it is possible to view how the flows vary after passing through the CLR reactor. The propane is totally converted and around 87% of the acetylene is converted as well, independently of the temperature. Table 15 displays the results obtained simulating the Gibbs reactor.

Table 15 - Gibbs reactor results

| Temperature                     | 750°C   |         |                      |                        | 800°C   |         |                      |                        |
|---------------------------------|---------|---------|----------------------|------------------------|---------|---------|----------------------|------------------------|
|                                 | In      | Out     | $\Delta_{Gibbs}$ [%] | $\Delta_{balance}$ [%] | In      | Out     | $\Delta_{Gibbs}$ [%] | $\Delta_{balance}$ [%] |
| $\dot{n}_{H_2}$                 | 0,01363 | 0,06105 | 348                  | 58                     | 0,01247 | 0,05448 | 337                  | 94                     |
| $\dot{n}_{CO}$                  | 0,01969 | 0,02380 | 21                   | -52                    | 0,01801 | 0,02311 | 28                   | -55                    |
| $\dot{n}_{CO_2}$                | 0,00915 | 0,02154 | 135                  | 117                    | 0,00837 | 0,01845 | 120                  | 141                    |
| $\dot{n}_{CH_4}$                | 0,00740 | 0,00008 | -99                  | 2                      | 0,00677 | 0,00002 | -100                 | 6                      |
| $\dot{n}_{C_2H_2}$              | 0,00022 | 0,00000 | -100                 | -88                    | 0,00020 | 0,00000 | -100                 | -86                    |
| $\dot{n}_{C_2H_4}$              | 0,00256 | 0,00000 | -100                 | -4                     | 0,00234 | 0,00000 | -100                 | -26                    |
| $\dot{n}_{C_2H_6}$              | 0,00023 | 0,00000 | -100                 | 3                      | 0,00021 | 0,00000 | -100                 | -67                    |
| $\dot{n}_{C_3H_8}$              | 0,00012 | 0,00000 | -100                 | -100                   | 0,00011 | 0,00000 | -100                 | -100                   |
| $\dot{n}_{N_2}$                 | 0,00667 | 0,00667 | 0                    | 0                      | 0,00610 | 0,00610 | 0                    | 22                     |
| $\dot{n}_{O_2 \text{ from AR}}$ | 0,00188 | 0,00000 | -100                 | -100                   | 0,00187 | 0,00000 | -100                 | -100                   |
| $\dot{n}_{tars}$                | 0,00028 | 0,00000 | -100                 | -8                     | 0,00026 | 0,00000 | -100                 | -30                    |
| $\dot{n}_{H_2O}$                | 0,06726 | 0,04212 | -37                  | -11                    | 0,06153 | 0,04001 | -35                  | -17                    |
| $\dot{n}_{He}$                  | 0,02162 | 0,02162 | 0                    | 0                      | 0,02040 | 0,02040 | 0                    | 0                      |

It is clearly visible that the Gibbs reactor flow variations vary significantly from the experiment. Therefore it cannot be used as a basis to represent of the CLR system.

The simulation with the Equilibrium reactor and water-gas shift and tar steam reforming equations implemented gives the following results:

Table 16 - Equilibrium reactor results without temperature approach

| Temperature                     | 750°C   |         |                    |                        | 800°C   |         |                    |                        |
|---------------------------------|---------|---------|--------------------|------------------------|---------|---------|--------------------|------------------------|
|                                 | In      | Out     | $\Delta_{Eq.}$ [%] | $\Delta_{balance}$ [%] | In      | Out     | $\Delta_{Eq.}$ [%] | $\Delta_{balance}$ [%] |
| $\dot{n}_{H_2}$                 | 0,01363 | 0,03028 | 122                | 58                     | 0,01247 | 0,02688 | 116                | 94                     |
| $\dot{n}_{CO}$                  | 0,01969 | 0,00976 | -50                | -52                    | 0,01801 | 0,00984 | -45                | -55                    |
| $\dot{n}_{CO_2}$                | 0,00915 | 0,02188 | 139                | 117                    | 0,00837 | 0,01914 | 129                | 141                    |
| $\dot{n}_{CH_4}$                | 0,00740 | 0,00740 | 0                  | 2                      | 0,00677 | 0,00677 | 0                  | 6                      |
| $\dot{n}_{C_2H_2}$              | 0,00022 | 0,00022 | 0                  | -88                    | 0,00020 | 0,00020 | 0                  | -86                    |
| $\dot{n}_{C_2H_4}$              | 0,00256 | 0,00256 | 0                  | -4                     | 0,00234 | 0,00234 | 0                  | -26                    |
| $\dot{n}_{C_2H_6}$              | 0,00023 | 0,00023 | 0                  | 3                      | 0,00021 | 0,00021 | 0                  | -67                    |
| $\dot{n}_{C_3H_8}$              | 0,00012 | 0,00012 | 0                  | -100                   | 0,00011 | 0,00011 | 0                  | -100                   |
| $\dot{n}_{N_2}$                 | 0,00667 | 0,00667 | 0                  | 0                      | 0,00610 | 0,00610 | 0                  | 22                     |
| $\dot{n}_{O_2 \text{ from AR}}$ | 0,00188 | 0,00188 | 0                  | -100                   | 0,00187 | 0,00187 | 0                  | -100                   |
| $\dot{n}_{tars}$                | 0,00028 | 0,00000 | -100               | -8                     | 0,00026 | 0,00000 | -100               | -30                    |
| $\dot{n}_{H_2O}$                | 0,06726 | 0,05173 | -23                | -11                    | 0,06153 | 0,04816 | -22                | -17                    |
| $\dot{n}_{He}$                  | 0,02162 | 0,02162 | 0                  | 0                      | 0,02040 | 0,02040 | 0                  | 0                      |

The calculated values are still very different from the experimental values. The tars are completely reformed because naphthalene is the representative compound, while in reality tars are a mix of different compounds, with naphthalene being only one of them.

In order to overcome this, the temperature approach methodology (section 4.5.) was applied to find a temperature difference ( $\Delta T$ ), and match the stream values. The concept of how the temperature approach works within ASPEN and in the reactor is explained in section 2.4. The results read:

Table 17 - Equilibrium reactor results with temperature approach

| Temperature                     | 750°C                            |         |                          |                           | 800°C                              |         |                          |                           |
|---------------------------------|----------------------------------|---------|--------------------------|---------------------------|------------------------------------|---------|--------------------------|---------------------------|
|                                 | $\Delta T = -1005^\circ\text{C}$ |         |                          |                           | $\Delta T = -469,63^\circ\text{C}$ |         |                          |                           |
| Flows<br>[mole/min]             | In                               | Out     | $\Delta T_{app.}$<br>[%] | $\Delta_{balance}$<br>[%] | In                                 | Out     | $\Delta T_{app.}$<br>[%] | $\Delta_{balance}$<br>[%] |
| $\dot{n}_{H_2}$                 | 0,01363                          | 0,00000 | -100                     | 58                        | 0,01247                            | 0,02408 | 93                       | 94                        |
| $\dot{n}_{CO}$                  | 0,01969                          | 0,00000 | -100                     | -52                       | 0,01801                            | 0,00832 | -54                      | -55                       |
| $\dot{n}_{CO_2}$                | 0,00915                          | 0,01496 | 64                       | 117                       | 0,00837                            | 0,01886 | 125                      | 141                       |
| $\dot{n}_{CH_4}$                | 0,00740                          | 0,00740 | 0                        | 2                         | 0,00677                            | 0,00677 | 0                        | 6                         |
| $\dot{n}_{C_2H_2}$              | 0,00022                          | 0,00022 | 0                        | -88                       | 0,00020                            | 0,00020 | 0                        | -86                       |
| $\dot{n}_{C_2H_4}$              | 0,00256                          | 0,00256 | 0                        | -4                        | 0,00234                            | 0,00234 | 0                        | -26                       |
| $\dot{n}_{C_2H_6}$              | 0,00023                          | 0,00023 | 0                        | 3                         | 0,00021                            | 0,00021 | 0                        | -67                       |
| $\dot{n}_{C_3H_8}$              | 0,00012                          | 0,00012 | 0                        | -100                      | 0,00011                            | 0,00011 | 0                        | -100                      |
| $\dot{n}_{N_2}$                 | 0,00667                          | 0,00667 | 0                        | 0                         | 0,00610                            | 0,00610 | 0                        | 22                        |
| $\dot{n}_{O_2 \text{ from AR}}$ | 0,00188                          | 0,00188 | 0                        | -100                      | 0,00187                            | 0,00187 | 0                        | -100                      |
| $\dot{n}_{tars}$                | 0,00028                          | 0,00167 | 487                      | -8                        | 0,00026                            | 0,00018 | -31                      | -30                       |
| $\dot{n}_{H_2O}$                | 0,06726                          | 0,07534 | 12                       | -11                       | 0,06153                            | 0,05024 | -18                      | -17                       |
| $\dot{n}_{He}$                  | 0,02162                          | 0,02162 | 0                        | 0                         | 0,02040                            | 0,02040 | 0                        | 0                         |

The temperature approach only worked with the 800°C case. Stream variations for the components involved in the implemented reactions reach values quite near the experimental case. Even assuming a  $\Delta T$  as low as -1005 K, it was not possible to fit the stream values.

Plug flow reactor simulations were expected to give the best results, as chemical dynamics are considered through the implementation of power-laws. It was also assured that the simulation had matching residence times with the experimental values. Results are summarized in Table 18:

Table 18 - Plug flow reactor with Naphthalene power law values

| Temperature                     | 750°C   |         |                               |                           | 800°C   |         |                               |                           |
|---------------------------------|---------|---------|-------------------------------|---------------------------|---------|---------|-------------------------------|---------------------------|
|                                 | In      | Out     | $\Delta k_{C_8H_{10}}$<br>[%] | $\Delta_{balance}$<br>[%] | In      | Out     | $\Delta k_{C_8H_{10}}$<br>[%] | $\Delta_{balance}$<br>[%] |
| $\dot{n}_{H_2}$                 | 0,01363 | 0,02399 | 76                            | 58                        | 0,01247 | 0,02099 | 68                            | 94                        |
| $\dot{n}_{CO}$                  | 0,01969 | 0,00933 | -53                           | -52                       | 0,01801 | 0,00950 | -47                           | -55                       |
| $\dot{n}_{CO_2}$                | 0,00915 | 0,01951 | 113                           | 117                       | 0,00837 | 0,01688 | 102                           | 141                       |
| $\dot{n}_{CH_4}$                | 0,00740 | 0,00740 | 0                             | 2                         | 0,00677 | 0,00677 | 0                             | 6                         |
| $\dot{n}_{C_2H_2}$              | 0,00022 | 0,00022 | 2                             | -88                       | 0,00020 | 0,00020 | 1                             | -86                       |
| $\dot{n}_{C_2H_4}$              | 0,00256 | 0,00256 | 0                             | -4                        | 0,00234 | 0,00234 | 0                             | -26                       |
| $\dot{n}_{C_2H_6}$              | 0,00023 | 0,00023 | -2                            | 3                         | 0,00021 | 0,00021 | -2                            | -67                       |
| $\dot{n}_{C_3H_8}$              | 0,00012 | 0,00012 | -2                            | -100                      | 0,00011 | 0,00011 | -2                            | -100                      |
| $\dot{n}_{N_2}$                 | 0,00667 | 0,00667 | 0                             | 0                         | 0,00610 | 0,00610 | 0                             | 22                        |
| $\dot{n}_{O_2 \text{ from AR}}$ | 0,00188 | 0,00188 | 0                             | -100                      | 0,00187 | 0,00187 | 0                             | -100                      |
| $\dot{n}_{tars}$                | 0,00028 | 0,00028 | 0                             | -8                        | 0,00026 | 0,00026 | 0                             | -30                       |
| $\dot{n}_{H_2O}$                | 0,06726 | 0,05690 | -15                           | -11                       | 0,06153 | 0,05302 | -14                           | -17                       |
| $\dot{n}_{He}$                  | 0,02162 | 0,02162 | 0                             | 0                         | 0,02040 | 0,02040 | 0                             | 0                         |

No tars are reformed using the chemical constant for naphthalene. Therefore, the iterative process described in section 4.5. is used to calculate a chemical constant that induces reforming. The results are shown in the next table:

Table 19 - Plug flow reactor with  $k_{tars}$  found through iterative process

| Temperature                     | 750°C   |         |                           |                           | 800°C   |         |                           |                           |
|---------------------------------|---|---------|---------------------------|---------------------------|---|---------|---------------------------|---------------------------|
|                                 | $k = 6 \times 10^{17} m^{0,3} kmol^{-0,1} s^{-1}$ |         |                           |                           | $k = 4,7 \times 10^{17} m^{0,3} kmol^{-0,1} s^{-1}$ |         |                           |                           |
| Flows<br>[mole/min]             | In  | Out     | $\Delta k_{iter.}$<br>[%] | $\Delta_{balance}$<br>[%] | In  | Out     | $\Delta k_{iter.}$<br>[%] | $\Delta_{balance}$<br>[%] |
| $\dot{n}_{H_2}$                 | 0,01363   | 0,02429 | 78                        | 58                        | 0,01247   | 0,02216 | 78                        | 94                        |
| $\dot{n}_{CO}$                  | 0,01969   | 0,00950 | -52                       | -52                       | 0,01801   | 0,01023 | -43                       | -55                       |
| $\dot{n}_{CO_2}$                | 0,00915   | 0,01953 | 114                       | 117                       | 0,00837   | 0,01695 | 102                       | 141                       |
| $\dot{n}_{CH_4}$                | 0,00740   | 0,00740 | 0                         | 2                         | 0,00677   | 0,00677 | 0                         | 6                         |
| $\dot{n}_{C_2H_2}$              | 0,00022   | 0,00022 | 0                         | -88                       | 0,00020   | 0,00020 | 0                         | -86                       |
| $\dot{n}_{C_2H_4}$              | 0,00256   | 0,00256 | 0                         | -4                        | 0,00234   | 0,00234 | 0                         | -26                       |
| $\dot{n}_{C_2H_6}$              | 0,00023   | 0,00023 | 0                         | 3                         | 0,00021   | 0,00021 | 0                         | -67                       |
| $\dot{n}_{C_3H_8}$              | 0,00012   | 0,00012 | 0                         | -100                      | 0,00011   | 0,00011 | 0                         | -100                      |
| $\dot{n}_{N_2}$                 | 0,00667   | 0,00667 | 0                         | 0                         | 0,00610   | 0,00610 | 0                         | 22                        |
| $\dot{n}_{O_2 \text{ from AR}}$ | 0,00188   | 0,00188 | 0                         | -100                      | 0,00187   | 0,00187 | 0                         | -100                      |
| $\dot{n}_{tars}$                | 0,00028   | 0,00026 | -8                        | -8                        | 0,00026   | 0,00018 | -31                       | -30                       |
| $\dot{n}_{H_2O}$                | 0,06726   | 0,05668 | -16                       | -11                       | 0,06153   | 0,05216 | -15                       | -17                       |
| $\dot{n}_{He}$                  | 0,02162   | 0,02162 | 0                         | 0                         | 0,02040   | 0,02040 | 0                         | 0                         |

Adapting the tar kinetics to the real outlet flow, gives ASPEN values that are not similar but follow the trend verified for the experimental results at a high rate. The streams that proceed from methane to propane in the previous tables, do not match at any level the experimental results, as expected, because no reaction involving them was included. Nevertheless, their stream value is one order of magnitude lower than the stream values from the components included in reactions and therefore the influence on the total flow value is low.

In the case of nitrogen, leakage from the AR to the FR explains why the stream increases in the balance case, while in the model it remains constant.

In conclusion, it is possible to affirm that for the tested hypothesis, the plug flow with the adapted chemical constant for both temperatures and the equilibrium reactor with temperature approach for 800°C describe the FR more accurately.

## 5.4. Energetic assessment

### 5.4.1. 60% Ilmenite / 40% Silica-sand and 1% oxygen in AR

For energetic calculations only the simulations that give similar results and trends in comparison to the experimental values are used (plug flow with the adapted chemical

constant for both temperatures and the equilibrium reactor with temperature approach for 800°C). For this reason, only the Ilmenite case is evaluated, using the experimental data and the simulation results and by “combusting” the following chemical energy carriers: H<sub>2</sub>, CO, CH<sub>4</sub>, C<sub>2</sub>H<sub>2</sub>, C<sub>2</sub>H<sub>4</sub>, C<sub>2</sub>H<sub>6</sub>, C<sub>3</sub>H<sub>8</sub> at the inlet and the outlet. Results are shown in the following table:

Table 20 - Chemical energy loss assessment

| Conditions                                     | 750°C         |                          | 800°C         |                          |                      |
|--|---------------|--------------------------|---------------|--------------------------|----------------------|
|  | Molar balance | Plug flow with adapted k | Molar balance | Plug flow with adapted k | Temperature approach |
| $\Delta H_{C_{inlet\ gases}}^{298\ K} [Watt]$  | 317,4         |                          | 290,3         |                          |                      |
| $\Delta H_{C_{outlet\ gases}}^{298\ K} [Watt]$ | 292,2         | 312,3                    | 271,7         | 292,7                    | 291,4                |
| $\Delta H_{CLR} [\%]$                          | -8,0          | -1,6                     | -6,4          | 0,8                      | 0,4                  |

In the experimental results and considering the mentioned chemical energy carriers, it is possible to conclude that a loss occurs in both cases. On the other hand, the same trend is only visible in the plug flow for 750°C but is still not as high as the experimental values. For the 750°C the trend is not followed at all. There is even an increase in chemical energy. The explanation relies in the fact that in the modeling only hydrogen was considered to take part in reactions. The other possible energy carrier flows remained unaltered. When comparing the molar flows, it seems to have no major influence as the flow value is one order of magnitude lower than the higher flows. So, from this short comparison, it is possible to verify that at an energetic level their contribution has to be taken into account. For e.g. when looking at the molar flow results, acetylene and propane are almost totally oxidized, while in the model not.

## 6. Conclusion

Molar balance was applied in both data sets, Ilmenite and Manganese. The Ilmenite results were appropriate to use for ASPEN implementation, as with these, more coherent results between experimental values and simulations were obtained.

It is clearly visible how the AR flow out is sensitive to variation of molar balance input values. However, it is not an input value for the ASPEN Plus model and so there is no demand for more accurate measurements.

In the Ilmenite case, 87% of the acetylene and 100% of propane are oxidized and this trend seems to be independent of temperature. Unfortunately at 700°C results are unclear and so it is not possible to assess if the same trend can be applied in a general way for these system operative conditions. Generally, methane doesn't suffer high flow variations.

At a molar balance level, it seemed reasonable only to include two reactions, tar steam reforming and water-gas shift, leading to values that follow the same trend values and are often quite similar comparing to the experimental results. However, when doing the energy analysis in section 5.4, it is verified that the flows in the model not included in any reaction, probably oxidation reactions, cannot be left out. Actually there is a chemical energy loss, while in the models they are low or there can even be an increase. This indicates that more reactions related to the main chemical energy carriers that initially were not considered have to be implemented, in order to make the model fit not only at a molar balance level but also in energetic terms.

Regarding the Manganese measurements, it seems that some kind of error was committed and/or wrong assumptions were made. For this catalyst, no possible measurement combination was found that gave a closed molar balance and at the same time respected the elaborated data selection criteria.

It was only possible to elaborate a coarse model for each system condition. The described methodologies were applied for each condition and always different system descriptive values were obtained (e.g. chemical constant for tar breakdown and  $\Delta T$  from temperature approach). Elaborating a CLR model that covers all possible system conditions remains a laborious task. Detailed knowledge about the system reaction kinetics (tar reforming, catalyst kinetics, equilibrium reactions involved, etc.) needs deeper investigation.

## Further works

The proposed model and methodology should be tested with new and more accurate measurements obtained from the CLR system. Recent experiments confirmed that the helium flow assumptions are correct and correspond to reality. Around 70-80% of the fluidizing helium leaves the system through the FR and these values are also almost reached with the made assumptions (Appendix VII). Nevertheless, applying the balance knowing beforehand how the helium is distributed between the reactors could also be a further improvement to the model.

Another important upgrade to the model would be the implementation of oxidization reactions for the considered chemical energy carriers, in order to fit both energy balances, from the models and the experimental data.

Finally, it should be attempted to implement in the Aspen Plus model the more complex tar decomposition scheme elaborated in the master thesis "Development of a tar decomposition model for application in a Chemical-looping reformer operated with raw gas from a biomass gasifier" .

## Bibliography

1. *Steam reforming model compounds of biomass gasification tars: conversion at different operating conditions and tendency towards coke formation.* **Coll, Roberto, et al., et al.** Tarragone : Fuel Processing Technology, 2001, Vol. 74.
2. *Study of steam reforming of toluene used as model compound of tar produced by biomass gasification.* **Swierczynski, D., Courson, C. and Kiennemann, A.** 2007, Chemical Engineering and Processing, pp. 508-513.
3. *Tar Formation and Destruction in a Fixed-Bed Reactor Simulating Downdraft Gasification: Equipment Development and Characterization of Tar-Cracking Products.* **Dabai, Fadimatu, et al., et al.** London : ACS Publications, 2010.
4. **Bridgwater, A. V.** The technical and economic feasibility of biomass gasification for power generation. *Fuel.* 1995, Vol. 74, pp. 631-653.
5. **Heyne, Stefan.** *Process Integration Opportunities for Synthetic Natural Gas (SNG) Production by Thermal Gasification of Biomass.* Göteborg : Heat and Power Technology Department of Energy and Environment Chalmers University of Technology, 2010. ISSN: 1404-7098.
6. *Hot Gas Removal of Tars, Ammonia, and Hydrogen Sulfide from Biomass Gasification Gas.* **Torres, Walter , Pansare, Sourabh S. and Goodwin Jr., James G.** 2007, Catalysis Reviews, pp. 407 — 456.
7. *Steam reforming of tar from a biomass gasification process over Ni/olivine catalyst using toluene as a model compound.* **Swierczynski, D., et al., et al.** 2007, Applied Catalysis, pp. 211-222.
8. **Lind, Fredrik, Seemann, Martin and Thunman, Henrik.** *Continuous Catalytic Tar Reforming of Biomass Derived Raw Gas Simultaneous Catalyst Regeneration.* Göteborg : Department of Energy and Environment, Chalmers University of Technology.
9. *Tar property, analysis, reforming mechanism and model for biomass gasification—An overview.* **Li, Chunshan and Suzuki, Kenzi.** 2009, Renewable and Sustainable Energy Reviews, pp. 594-604.
10. **Milne, T.A, Evans, R.J. and Abatzoglou, N.** *Biomass Gasifier “Tars”: Their Nature, Formation and Conversion.* s.l. : National Renewable Energy Laboratory, 1998.
11. **Hayes, R E, Thomas, W J and Hayes, K E.** A study of the nickel-catalyzed methanation reaction. *Journal of Catalysis.* 2, 1985, Vol. 92, pp. 312-326.

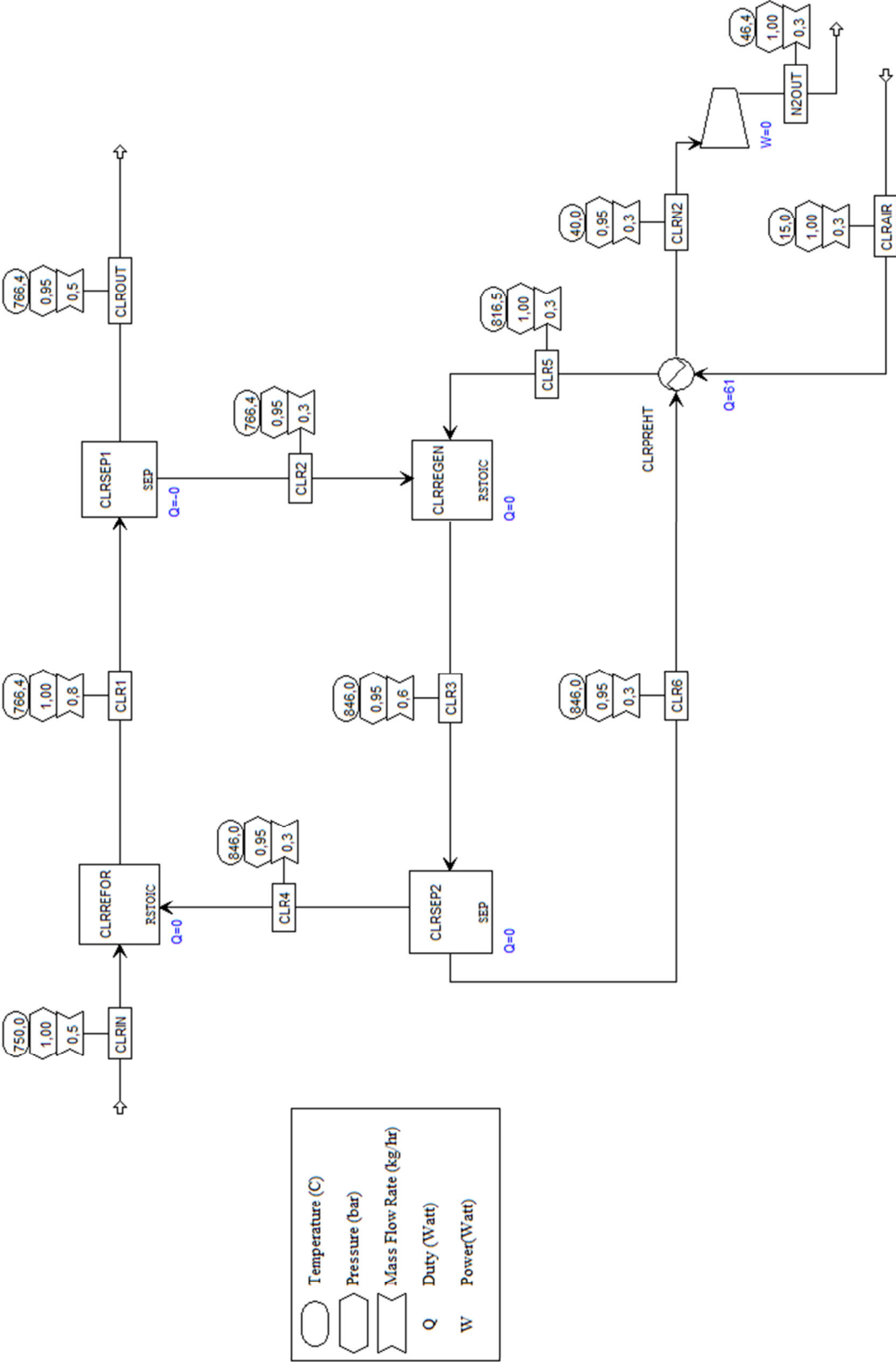
12. **Rapagnà, S., et al., et al.** Steam-gasification of biomass in a fluidised-bed of olivine particles. *Biomass and Bioenergy*. s.l. : Elsevier Science B.V., 2000, Vol. 19, pp. 187-197.
13. **Simell, Pekka A.** Effects of gasification gas components on tar and ammonia decomposition over hot gas cleanup catalysts. *Fuel*. 1997, Vol. 76, pp. 1117-1127.
14. **Mendiara, Teresa.** *Chemical Looping Reforming of Generator Gas*. Department of Chemical and Biomchemical Engineering. Lyngby, Denmark : s.n., 2009.
15. **Aspen Tech.** Getting Started Building and Running a Process Model. 2006.5. s.l. : Aspen Tech, 2007.
16. **Van Ness, Hendrick C. and Abbott, C. M.** Thermodynamics. [book auth.] R. H. Perry and D. W. Green. *Perry's Chemical Engineers' Handbook*. 7th. s.l. : McGraw-Hill, 1997.
17. *Modeling the Thermal Destruction of Toluene (C<sub>7</sub>H<sub>8</sub>) as Tar-Related Species for Fuel Gas Cleanup*. **Taralas, Georgios, Kontominas, Michael G. and Kakatsios, Xenophon.** 2003, Energy & Fuels, pp. 329-337.
18. *Fresh Tar (from a Biomass Gasifier) Elimination over a Commercial Steam-Reforming Catalyst. Kinetics and Effect of Different Variables of Operation*. **Narváez, Ian, Corella, José and Orío, Alberto.** 1997, Industrial & Engineering Chemistry Research, pp. 317-327.
19. **Fjellerup, Jan, et al., et al.** *Formation, Decomposition and Cracking of Biomass Tars in Gasification*. s.l. : Technical University of Denmark, 2005.
20. **Dayton, D.** *A Review of the Literature on Catalytic Biomass Tar Destruction*. s.l. : National Renewable Energy Laboratory, 2002.
21. *Improving the Modeling of the Kinetics of the Catalytic Tar Elimination in Biomass Gasification*. **Corella, José, Toledo, José M. and Aznar, Maria-Pilar.** 2002, Industrial & Engineering Chemistry Research, pp. 3351-3356.
22. **Thunman, Henrik , Lind, Fredrik and Seemann, Martin.** Tar Cleaning with Chemical Looping Reforming.
23. **Ryden, M., Lyngfelt, A. and Mattisson, T.** Synthesis gas generation by chemical-looping reforming in a continuously operating laboratory reactor. *Fuel*. 12-13. 2006, Vol. 85, pp. 1631-1641.
24. **Corella, José, Orío, Alberto and Aznar , Pilar.** Biomass Gasification with Air in Fluidized Bed: Reforming of the Gas Composition with Commercial Steam Reforming Catalysts. *Industrial Engineering Chemistry Research*. s.l. : American Chemical Society, 1998, pp. 4617-4624.

25. Getting Started Building and Running a Process Model. 2006.5. s.l. : Aspen Tech, 2007.

26. **Walas, Stanley W.** Reaction Kinetics. [book auth.] R.H. Perry and D.W. Green. *Perry's Chemical Engineers' Handbook*. 7th. s.l. : McGraw-Hill, 1997.

27. ERA-NET final report.

# Appendix I – Old Aspen Plus CLR flow-sheet



## Appendix II – MatLab file for molar balance

```
%=====
%
%                               BALANCES
%
%=====
clear all
clc
% CALL THE EXCEL FILE
filename = 'Concentrations_for_MatLab.xls';
open = xlsread(filename);

% SPECIES CONCENTRATIONS [%mol]

conc_FR_in = open(91:107,29:39); % [H2, CO, CO2, CH4, C2H2, C2H4, C2H6, C3H8, N2]
size_FR_in = size(conc_FR_in);

conc_FR_out_700 = open(11:28,29:39);
% [H2, CO, CO2, CH4, C2H2, C2H4, C2H6, C3H8, N2, O2, He]
size_FR_700 = size(conc_FR_out_700);

conc_FR_out_750 = open(34:53,29:39);
% [H2, CO, CO2, CH4, C2H2, C2H4, C2H6, C3H8, N2, O2, He]
size_FR_750 = size(conc_FR_out_750);

conc_FR_out_800 = open(59:72,29:39);
% [H2, CO, CO2, CH4, C2H2, C2H4, C2H6, C3H8, N2, O2, He]
size_FR_800 = size(conc_FR_out_800);

conc_AR_out_700 = open(118:3564,4:5); % [CO2, O2]
size_AR_700 = size(conc_AR_out_700);

conc_AR_out_750 = open(3564:7185,4:5); % [CO2, O2]
size_AR_750 = size(conc_AR_out_750);

conc_AR_out_800 = open(7186:9829,4:5); % [CO2, O2]
size_AR_800 = size(conc_AR_out_800);

H2O_in = open(14,43); % [g/l]
Tars_in = open(9,43); % [g/l]
Tars_out_700 = open(9,44); % [g/l]
Tars_out_750 = open(27,44); % [g/l]
Tars_out_800 = open(45,44); % [g/l]

% FLOWS

v_dry_out = open(14,44); % [l/min]
He_SLS = open(60,44); % [l/min]
He_ILS = open(61,44); % [l/min]
He_in = He_SLS+He_ILS; % [l/min]
O2_AR_in = open(65,44); % [l/min]
N2_AR_in = open(66,44); % [l/min]

clear open
```

```

% Constants

%Molar Volume
Vm = 22.4; % [l/mole]

%Molar weights

H2 = 2; % [g/mole]
CO = 28; % [g/mole]
CO2 = 44; % [g/mole]
CH4 = 16; % [g/mole]
C2H2 = 26; % [g/mole]
C2H4 = 28; % [g/mole]
C2H6 = 30; % [g/mole]
C3H8 = 44; % [g/mole]
N2 = 28; % [g/mole]
O2 = 32; % [g/mole]
H2O = 18; % [g/mole]

%Considering Naphtalene (C10H8)
Tars = 128; % [g/mole]

%Moles of each species in each molecules
% [H2, CO, CO2, CH4, C2H2, C2H4, C2H6, C3H8, N2, O2, He]
%Carbon
moles_C = [0 1 1 1 2 2 2 3 0 0 0];
%Hidrogen
moles_H = [2 0 0 4 2 4 6 8 0 0 0];
%Oxygen
moles_O = [0 1 2 0 0 0 0 0 0 2 0];
%Nitrogen
moles_N = [0 0 0 0 0 0 0 0 2 0 0];

% CALCULATIONS

%Average FR input concentration

av_con_FR_in = sum(conc_FR_in,1)/size_FR_in(1,1);

%%%%%%%%%%%%%%%%%%%%%%%%%%%%%%%%%%%%%%%%%%%%%%%%%%%%%%%%%%%%%%%%%%%%%%%%%%

%LOOPS TO FIND OUT n_FR_in_dry, n_FR_out_H2O and n_AR_out (molar flows)

%%%%%%%%%%%%%%%%%%%%%%%%%%%%%%%%%%%%%%%%%%%%%%%%%%%%%%%%%%%%%%%%%%%%%%%%%%

% Matrix M and vector a

M = [0 0 0 ; 0 -2 0 ; 0 -1 0 ];
a = zeros(3,1);

%Auxiliar vector for in FR concentrations

inFR = av_con_FR_in;

%Creates Excel file to write results

Matrix_scheme = {'[mol/min],[%mol/mol] and [-]' 'H2' 'CO' 'CO2' 'CH4'
' C2H2' 'C2H4' 'C2H6' 'C3H8' 'N2'...

```

```

'O2 from AR' 'He' 'Tars' 'H2O' 'Dry flow(out is with He)' 'Humid
flow(out is with He)'...
'C' 'H' 'O' 'N' 'AR' 'N2 AR out-balance' 'N2 AR out-He' 'sigma' '[CO2
out AR]' '[O2 out AR]' 'location FR out list' 'location AR out list';

xlswrite('Flow Results',Matrix_scheme,'700','A1');
xlswrite('Flow Results',Matrix_scheme,'750','A1');
xlswrite('Flow Results',Matrix_scheme,'800','A1');

Matrix_scheme = {'Average in Concentrations[%]'};

xlswrite('Flow Results',Matrix_scheme,'700','A3');
xlswrite('Flow Results',Matrix_scheme,'750','A3');
xlswrite('Flow Results',Matrix_scheme,'800','A3');
xlswrite('Flow Results',inFR,'700','B3');
xlswrite('Flow Results',inFR,'750','B3');
xlswrite('Flow Results',inFR,'800','B3');

Matrix_scheme = {'Flow in FR[mol/min]'};

xlswrite('Flow Results',Matrix_scheme,'700','A5');
xlswrite('Flow Results',Matrix_scheme,'750','A5');
xlswrite('Flow Results',Matrix_scheme,'800','A5');

Matrix_scheme = {'Flow out FR[mol/min]'};

xlswrite('Flow Results',Matrix_scheme,'700','A6');
xlswrite('Flow Results',Matrix_scheme,'750','A6');
xlswrite('Flow Results',Matrix_scheme,'800','A6');

Matrix_scheme = {'[Concentrations out FR(1-9,11),AR(21-22) and N2 balance
out AR[mol/min]]'};

xlswrite('Flow Results',Matrix_scheme,'700','A7');
xlswrite('Flow Results',Matrix_scheme,'750','A7');
xlswrite('Flow Results',Matrix_scheme,'800','A7');

%%%%%%%%%%%%%%%%%%%%%%%%%%%%%%%%%%%%%%%%%%%%%%%%%%%%%%%%%%%%%%%%%%%%%%%%

% loop for 700 degrees Celsius

Tars_out = Tars_out_700;

%Result matrix and auxiliar writing variable
results700 = zeros(size_FR_700(1,1)*size_AR_700(1,1),7);
Results_Excel = zeros(1,24);
h = 0;
k = 0;
calc_dec = 0;

for i = 1:size_FR_700(1,1)

    %Auxiliar vector for out FR concentrations
    outFR = conc_FR_out_700(i,:);

    %jumps AR concentrations as they repeat itself

```

```

for j = 1:2:size_AR_700(1,1)

    %Auxiliar vector for out AR concentrations
    outAR = conc_AR_out_700(j,:);

    calc_dec = calc_dec-sum(outAR);

    if calc_dec ~= 0

        calc_dec = sum(outAR);

        %Carbon balance coefficients
        M(1,1) = (inFR*moles_C')/100 + 10*Tars_in*Vm/Tars;

        M(1,3) = -outAR(1)/100;

        a(1,1) = (v_dry_out/Vm)*((outFR*moles_C')/100 +
10*Tars_out*Vm/Tars);

        %Hydrogen balance coefficients

        M(2,1) = (inFR*moles_H')/100 + 8*Tars_in*Vm/Tars +
2*H2O_in*Vm/H2O;

        a(2,1) = (v_dry_out/Vm)*((outFR*moles_H')/100 +
8*Tars_out*Vm/Tars);

        %Oxigen balance coefficients

        M(3,1) = (inFR*moles_O')/100 + H2O_in*Vm/H2O;

        M(3,3) = -2*(outAR(1)+outAR(2))/100;

        a(3,1) = (v_dry_out/Vm)*(outFR*moles_O')/100 - 2*O2_AR_in/Vm;

        %Calculates flows

        n = M\a;

        %Writes realistic results

        if n(3) > 0
            h = h+1;
            results700(h,1) = n(1);
            results700(h,2) = n(2);
            results700(h,3) = n(3);

            %AR flow out with different units [l/m]
            results700(h,4)=n(3)*Vm;

            %AR flow in to compare with AR flow out result
            results700(h,5)=(He_SLS+He_ILS)*(1-
outFR(11)/100)+O2_AR_in+N2_AR_in;

            %Writes location of AR_out and FR_out
            results700(h,6)=i;

```

```

results700(h,7)=j;

%Writes results and information into excel file [n/min]-
line 1 in and line 2 out

k = k+1;

Results_Excel(k,1:11) = inFR*n(1)/100;
Results_Excel(k,10) = O2_AR_in/Vm-n(3)*(sum(outAR))/100;
Results_Excel(k,11) = (outFR(11)/100)*v_dry_out/Vm;
Results_Excel(k,12) = n(1)*Tars_in*Vm/Tars;
Results_Excel(k,13) = n(1)*H2O_in*Vm/H2O;
Results_Excel(k,14) =
sum(Results_Excel(k,1:9))+Results_Excel(k,10)...
+Results_Excel(k,12);
Results_Excel(k,15) =
Results_Excel(k,14)+Results_Excel(k,13);
Results_Excel(k,16) = Results_Excel(k,1:11)*moles_C'...
+10*Results_Excel(k,12);
Results_Excel(k,17) = Results_Excel(k,1:11)*moles_H'...
+8*Results_Excel(k,12)+2*Results_Excel(k,13);
Results_Excel(k,18) = Results_Excel(k,1:11)*moles_O'...
+Results_Excel(k,13);
Results_Excel(k,19) = Results_Excel(k,1:11)*moles_N';
Results_Excel(k,20) = ((He_SLS+He_ILS)*(1-
outFR(11)/100)+O2_AR_in...
+N2_AR_in)/Vm;

k = k+1;

Results_Excel(k,1:11) = outFR*(v_dry_out/Vm)/100;
Results_Excel(k,10) = 0;
Results_Excel(k,11) = (outFR(11)/100)*v_dry_out/Vm;
Results_Excel(k,12) = (v_dry_out/Vm)*Tars_out*Vm/Tars;
Results_Excel(k,13) = n(2);
Results_Excel(k,14) =
sum(Results_Excel(k,1:9))+Results_Excel(k,10)...
+Results_Excel(k,11)+Results_Excel(k,12);
Results_Excel(k,15) =
Results_Excel(k,14)+Results_Excel(k,13);
Results_Excel(k,16) = Results_Excel(k,1:11)*moles_C'...
+10*Results_Excel(k,12);
Results_Excel(k,17) = Results_Excel(k,1:11)*moles_H'...
+8*Results_Excel(k,12)+2*Results_Excel(k,13);
Results_Excel(k,18) = Results_Excel(k,1:11)*moles_O'...
+Results_Excel(k,13);
Results_Excel(k,19) = Results_Excel(k,1:11)*moles_N';
Results_Excel(k,20) = n(3);

k = k+1;

%Writes FR and AR out concentrations and [mol/min] N2
balance

Results_Excel(k,1:11) = outFR;
Results_Excel(k,21) = (N2_AR_in/Vm+inFR(9)*n(1)/100)-...
outFR(9)*v_dry_out/(100*Vm);
Results_Excel(k,22) = n(3)*(1-sum(outAR)/100)-...
(He_in-v_dry_out*(1-sum(outFR)/100))/Vm;
Results_Excel(k,23) = (1-Results_Excel(k,22))/...

```

```

        Results_Excel(k,21))*100;
Results_Excel(k,24:25) = outAR;
Results_Excel(k,26) = i;
Results_Excel(k,27) = j;

    k = k+1;

        else
        end
    else
    end
end
end

%results700 = Results_Excel;

%Write in Excel file
xlswrite('Flow Results',Results_Excel,'700','B5');
clear Results_Excel;

```

..... (Note: Code only for 700°C is shown, as for the other temperatures it is the same.)





|     | B          | C        | D         | E    |
|-----|------------|----------|-----------|------|
| 112 |            |          |           |      |
| 113 |            |          | AR Outlet |      |
| 114 |            |          |           |      |
| 115 |            |          |           |      |
| 116 |            |          |           |      |
| 117 |            |          | %CO2      | %O2  |
| 118 | 2010-03-25 | 09:58:35 | 0,13      | 0,26 |
| 119 | 2010-03-25 | 09:58:36 | 0,13      | 0,25 |
| 120 | 2010-03-25 | 09:58:37 | 0,13      | 0,25 |
| 121 | 2010-03-25 | 09:58:38 | 0,13      | 0,25 |
| 122 | 2010-03-25 | 09:58:39 | 0,13      | 0,25 |
| 123 | 2010-03-25 | 09:58:40 | 0,13      | 0,23 |
| 124 | 2010-03-25 | 09:58:41 | 0,13      | 0,23 |
| 125 | 2010-03-25 | 09:58:42 | 0,13      | 0,23 |
| 126 | 2010-03-25 | 09:58:43 | 0,13      | 0,23 |
| 127 | 2010-03-25 | 09:58:44 | 0,13      | 0,22 |
| 128 | 2010-03-25 | 09:58:45 | 0,13      | 0,22 |
| 129 | 2010-03-25 | 09:58:46 | 0,13      | 0,2  |
| 130 | 2010-03-25 | 09:58:47 | 0,13      | 0,2  |
| 131 | 2010-03-25 | 09:58:48 | 0,13      | 0,2  |
| 132 | 2010-03-25 | 09:58:49 | 0,13      | 0,2  |
| 133 | 2010-03-25 | 09:58:50 | 0,13      | 0,2  |
| 134 | 2010-03-25 | 09:58:51 | 0,13      | 0,2  |
| 135 | 2010-03-25 | 09:58:52 | 0,14      | 0,19 |
| 136 | 2010-03-25 | 09:58:53 | 0,14      | 0,19 |
| 137 | 2010-03-25 | 09:58:54 | 0,13      | 0,19 |
| 138 | 2010-03-25 | 09:58:55 | 0,13      | 0,19 |
| 139 | 2010-03-25 | 09:58:56 | 0,14      | 0,19 |
| 140 | 2010-03-25 | 09:58:57 | 0,14      | 0,19 |
| 141 | 2010-03-25 | 09:58:58 | 0,13      | 0,19 |
| 142 | 2010-03-25 | 09:58:59 | 0,13      | 0,19 |
| 143 | 2010-03-25 | 09:59:00 | 0,14      | 0,18 |
| 144 | 2010-03-25 | 09:59:01 | 0,14      | 0,18 |
| 145 | 2010-03-25 | 09:59:02 | 0,13      | 0,18 |
| 146 | 2010-03-25 | 09:59:03 | 0,13      | 0,18 |
| 147 | 2010-03-25 | 09:59:04 | 0,14      | 0,18 |
| 148 | 2010-03-25 | 09:59:05 | 0,14      | 0,18 |
| 149 | 2010-03-25 | 09:59:06 | 0,14      | 0,18 |
| 150 | 2010-03-25 | 09:59:07 | 0,14      | 0,18 |
| 151 | 2010-03-25 | 09:59:08 | 0,14      | 0,17 |
| 152 | 2010-03-25 | 09:59:09 | 0,14      | 0,17 |
| 153 | 2010-03-25 | 09:59:10 | 0,13      | 0,16 |
| 154 | 2010-03-25 | 09:59:11 | 0,13      | 0,16 |
| 155 | 2010-03-25 | 09:59:12 | 0,13      | 0,17 |
| 156 | 2010-03-25 | 09:59:13 | 0,13      | 0,17 |
| 157 | 2010-03-25 | 09:59:14 | 0,13      | 0,17 |

|    | AQ             | AR              |
|----|----------------|-----------------|
| 1  |                |                 |
| 2  |                |                 |
| 3  |                |                 |
| 4  |                |                 |
| 5  | 700            |                 |
| 6  | Tars IN (g/m3) | Tars OUT (g/m3) |
| 7  | 27,24          | 26,41           |
| 8  | (g/l)          | (g/l)           |
| 9  | 0,02724        | 0,02641         |
| 10 |                |                 |
| 11 |                |                 |
| 12 |                |                 |
| 13 | H2O IN (g/l)   | flow OUT(l/min) |
| 14 | 0,905845477    | 2               |
| 15 |                |                 |
| 16 |                |                 |
| 17 |                |                 |
| 18 | AR             |                 |
| 19 | O2 IN (l/min)  | N2 IN (l/min)   |
| 20 | 0,0546         | 5,2454          |
| 21 |                |                 |
| 22 |                |                 |
| 23 | 750            |                 |
| 24 | Tars IN (g/m3) | Tars OUT (g/m3) |
| 25 | 27,24          | 16,78           |
| 26 | (g/l)          | (g/l)           |
| 27 | 0,02724        | 0,01678         |
| 28 |                |                 |
| 29 |                |                 |
| 30 |                |                 |
| 31 | H2O IN (g/l)   |                 |
| 32 | 0,905845477    |                 |
| 33 |                |                 |
| 34 |                |                 |
| 35 |                |                 |
| 36 | AR             |                 |
| 37 | O2 IN (l/min)  | N2 IN (l/min)   |
| 38 | 0,0546         | 5,2454          |
| 39 |                |                 |
| 40 |                |                 |
| 41 | 800            |                 |
| 42 | Tars IN (g/m3) | Tars OUT (g/m3) |
| 43 | 27,24          | 11,74           |
| 44 | (g/l)          | (g/l)           |
| 45 | 0,02724        | 0,01174         |
| 46 |                |                 |
| 47 |                |                 |
| 48 |                |                 |
| 49 | H2O IN (g/l)   |                 |
| 50 | 0,905845477    |                 |
| 51 |                |                 |
| 52 |                |                 |
| 53 |                |                 |
| 54 | AR             |                 |
| 55 | O2 IN (l/min)  | N2 IN (l/min)   |
| 56 | 0,0546         | 5,2454          |
| 57 |                |                 |

## Manganese

Note: The data for the Manganese input is organized in the same way as in the Ilmenite data.

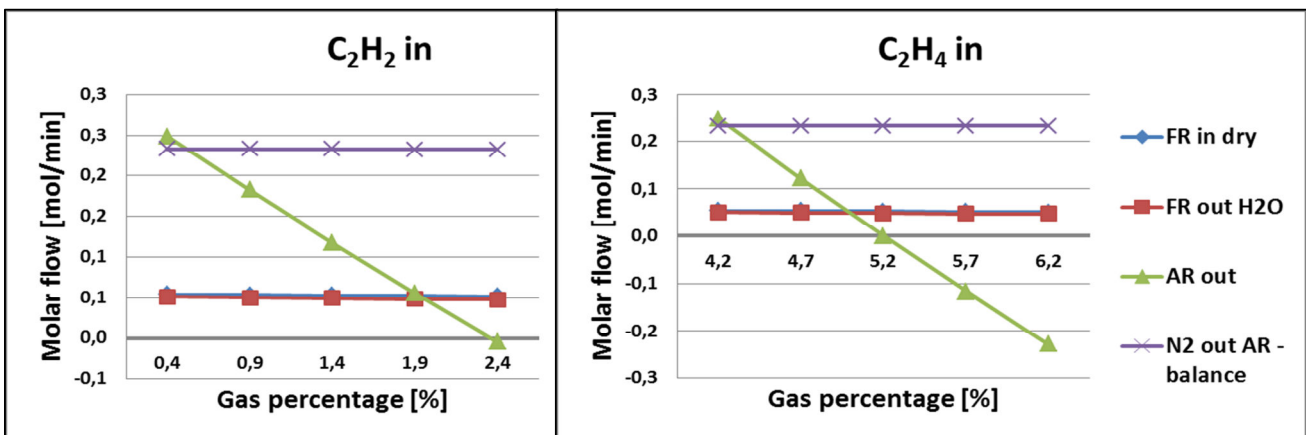
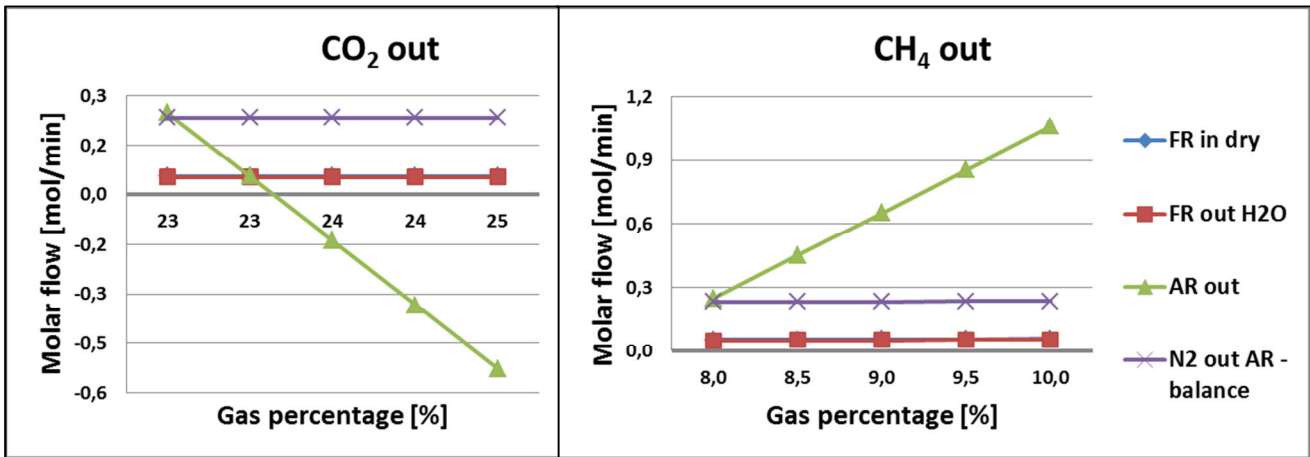
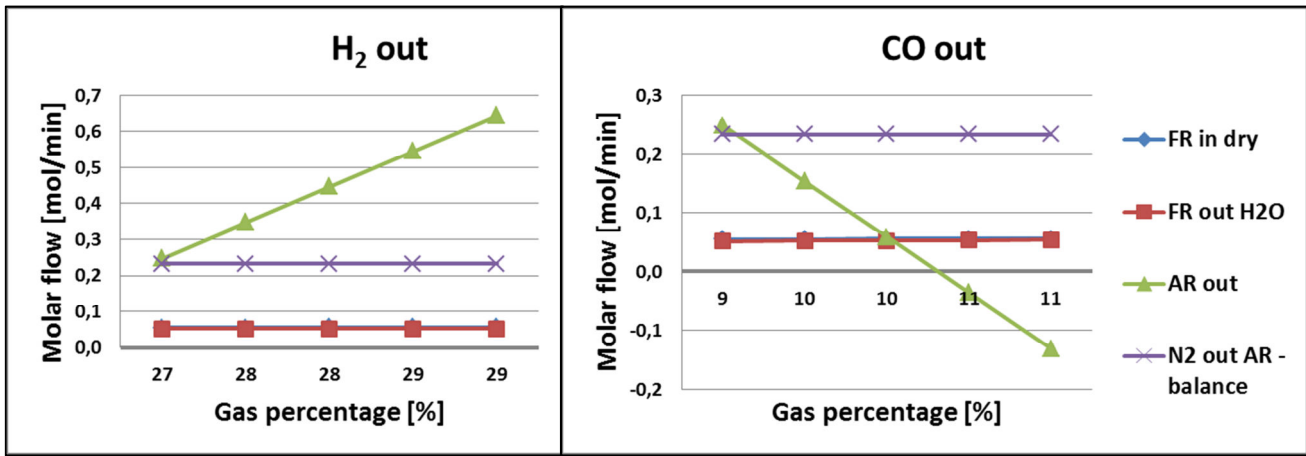
# Appendix IV – MatLab results example

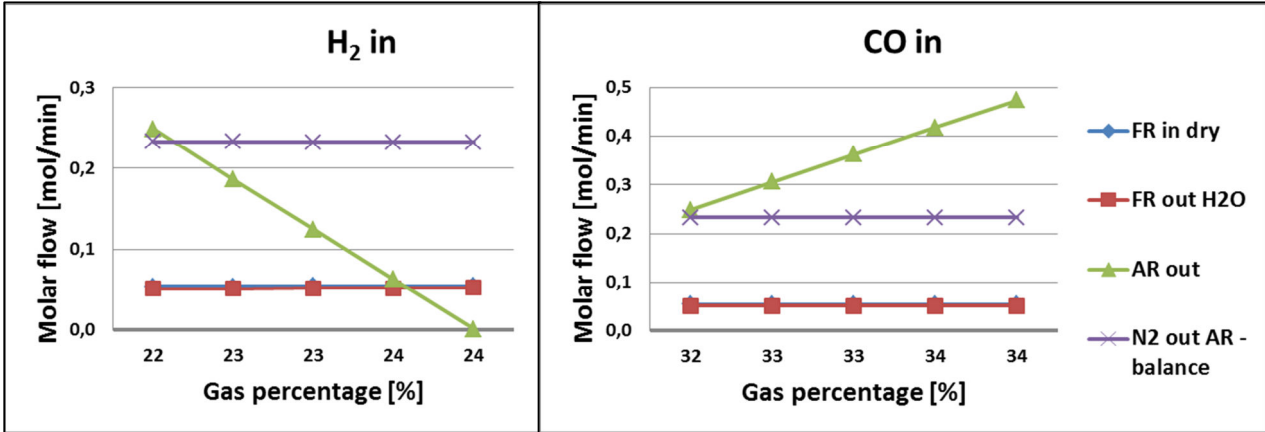
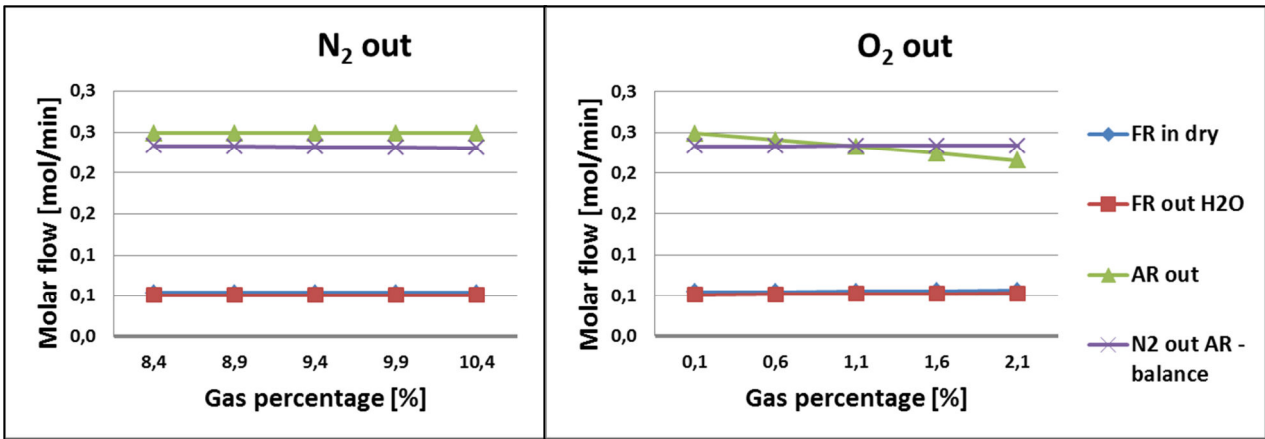
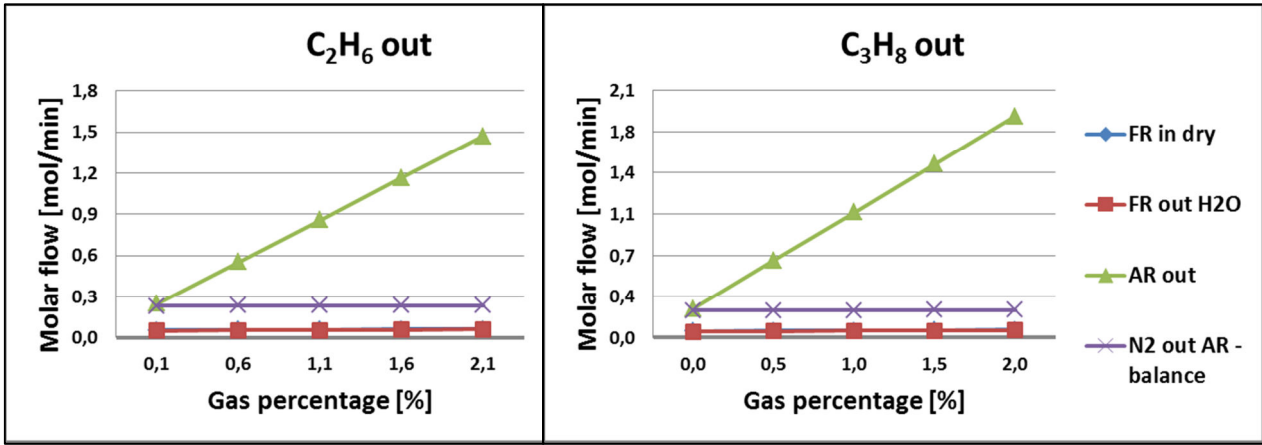
|   | A   | B       | C       | D       | E       | F       | G       |
|---|---|---------|---------|---------|---------|---------|---------|
| 1 | [mol/min],[%mol/mol] and [-]  | H2      | CO      | CO2     | CH4     | C2H2    | C2H4    |
| 2 |   |         |         |         |         |         |         |
| 3 | Average in Concentrations[%]  | 22,84   | 32,99   | 15,33   | 12,40   | 0,36    | 4,29    |
| 4 |   |         |         |         |         |         |         |
| 5 | Flow in FR[mol/min]   | 0,01357 | 0,01960 | 0,00911 | 0,00737 | 0,00022 | 0,00255 |
| 6 | Flow out FR[mol/min]  | 0,02296 | 0,00946 | 0,02069 | 0,00772 | 0,00004 | 0,00214 |
| 7 | Concentrations out FR(1-9,11),AR(21-22) and N2 balance out AR[mol/mi] | 25,72   | 10,60   | 23,18   | 8,65    | 0,04    | 2,40    |

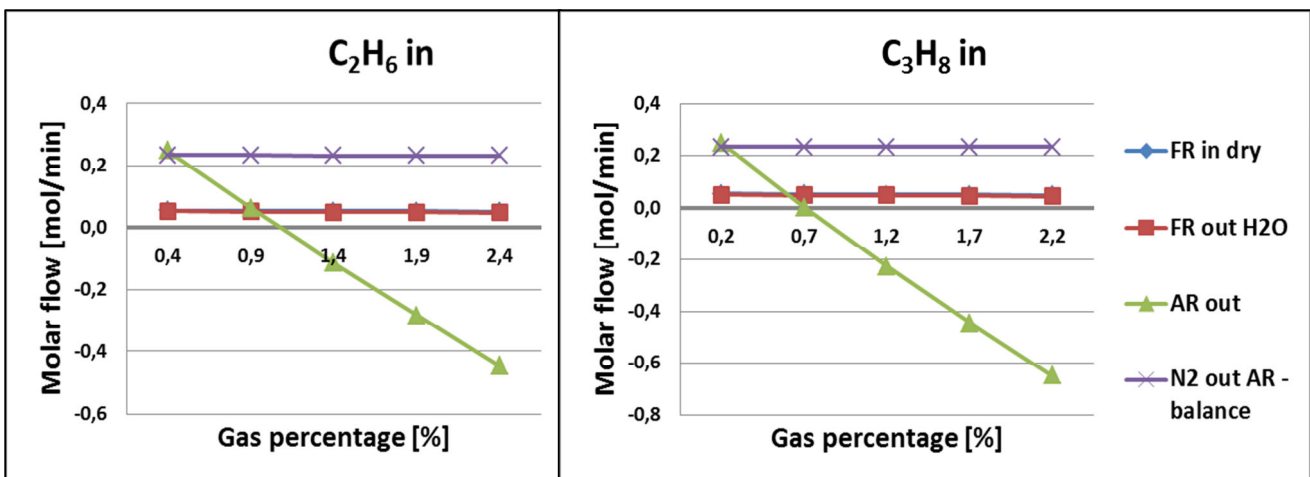
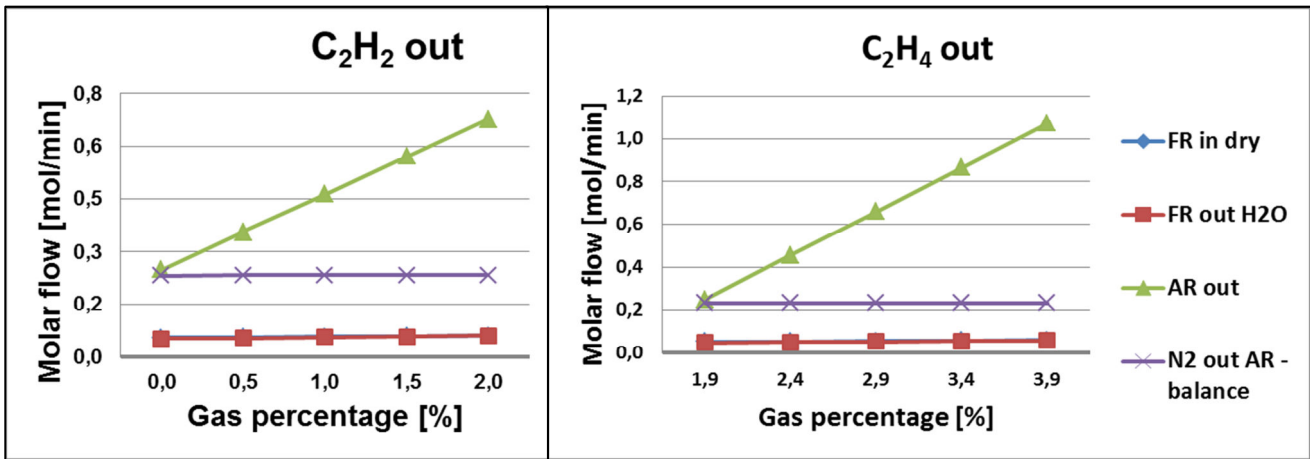
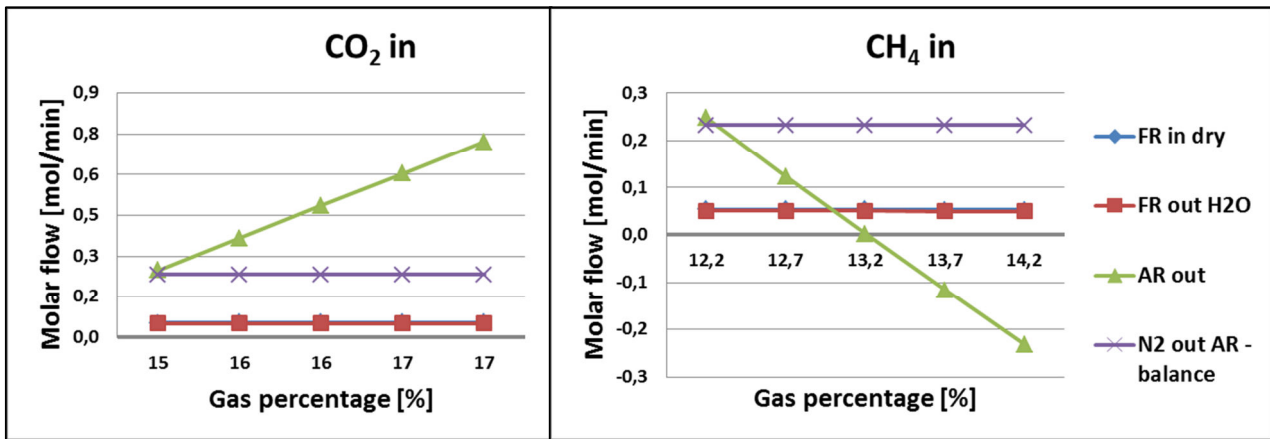
|   | G       | H       | I       | J       | K          | L       | M       | N       | O                        | P                          |
|---|---------|---------|---------|---------|------------|---------|---------|---------|--------------------------|----------------------------|
| 1 | C2H4    | C2H6    | C3H8    | N2      | O2 from AR | He      | Tars    | H2O     | Dry flow(out is with He) | Humid flow(out is with He) |
| 2 |         |         |         |         |            |         |         |         |                          |                            |
| 3 | 4,29    | 0,39    | 0,21    | 11,17   | 0          | 100     |         |         |                          |                            |
| 4 |         |         |         |         |            |         |         |         |                          |                            |
| 5 | 0,00255 | 0,00023 | 0,00012 | 0,00664 | 0,00212    | 0,01962 | 0,00028 | 0,06698 | 0,06182                  | 0,12880                    |
| 6 | 0,00214 | 0,00012 | 0,00023 | 0,00631 | 0,00000    | 0,01962 | 0,00018 | 0,05820 | 0,08947                  | 0,14767                    |
| 7 | 2,40    | 0,13    | 0,26    | 7,06    |            | 21,97   |         |         |                          |                            |

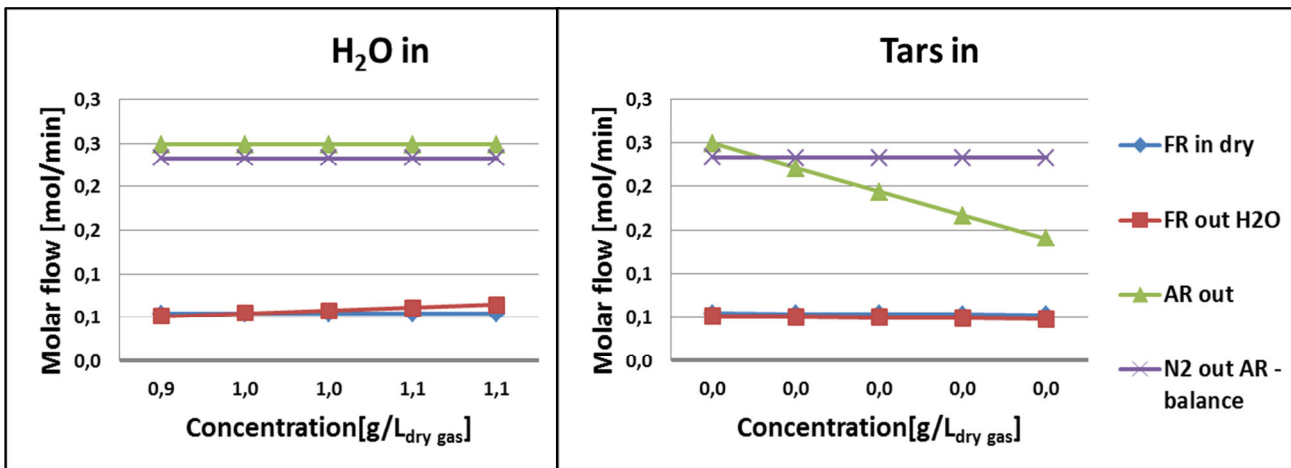
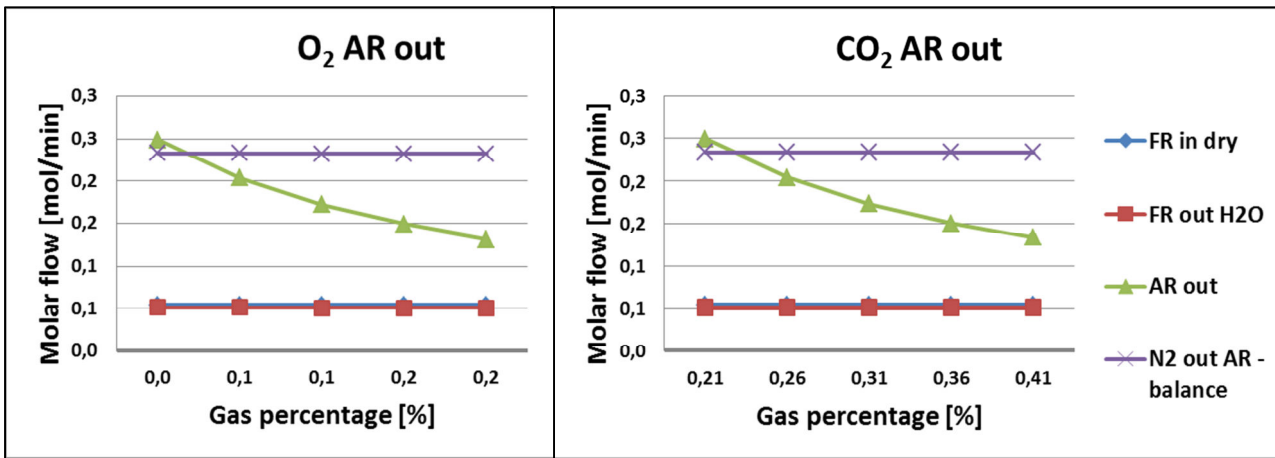
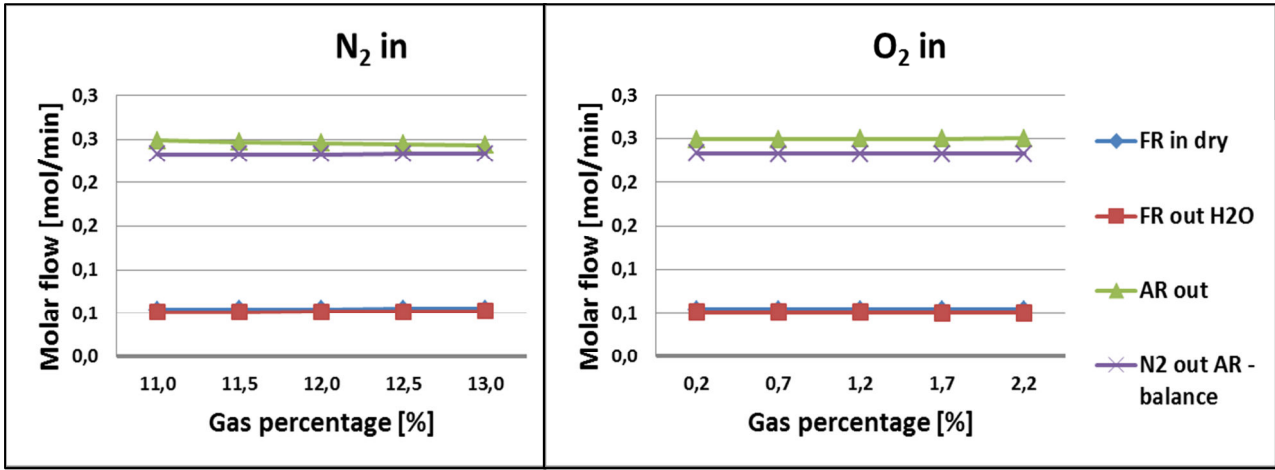
|   | Q       | R       | S       | T       | U       | V                 | W            | X       | Y            | Z         | AA                   | AB                   |
|---|---------|---------|---------|---------|---------|-------------------|--------------|---------|--------------|-----------|----------------------|----------------------|
| 1 | C       | H       | O       | N       | AR      | N2 AR out-balance | N2 AR out-He | sigma   | [CO2 out AR] | O2 out AR | location FR out list | location AR out list |
| 2 |         |         |         |         |         |                   |              |         |              |           |                      |                      |
| 3 |         |         |         |         |         |                   |              |         |              |           |                      |                      |
| 4 |         |         |         |         |         |                   |              |         |              |           |                      |                      |
| 5 | 0,04529 | 0,20587 | 0,10905 | 0,01328 | 0,25611 |                   |              |         |              |           |                      |                      |
| 6 | 0,04500 | 0,20587 | 0,10905 | 0,01261 | 0,13808 |                   |              |         |              |           |                      |                      |
| 7 |         |         |         |         |         | 0,23450044        | 0,112760114  | 51,9148 | 0,21         | 0,02      | 1                    | 1                    |

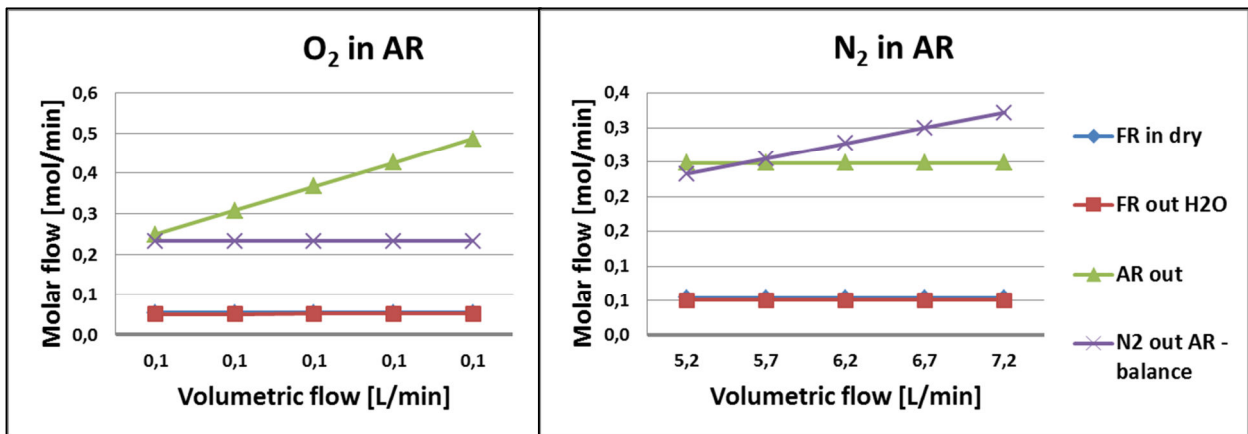
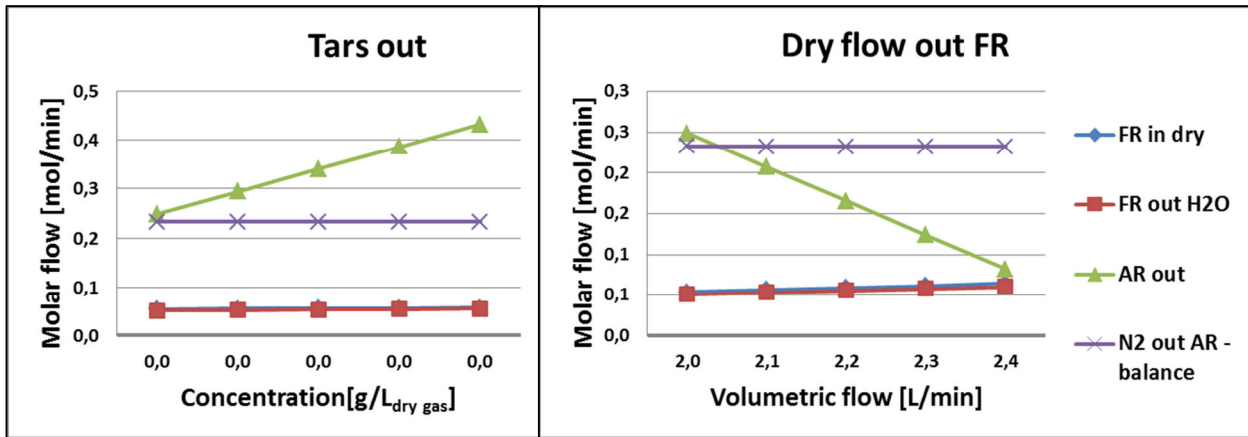
# Appendix V – Sensitivity analysis Ilmenite







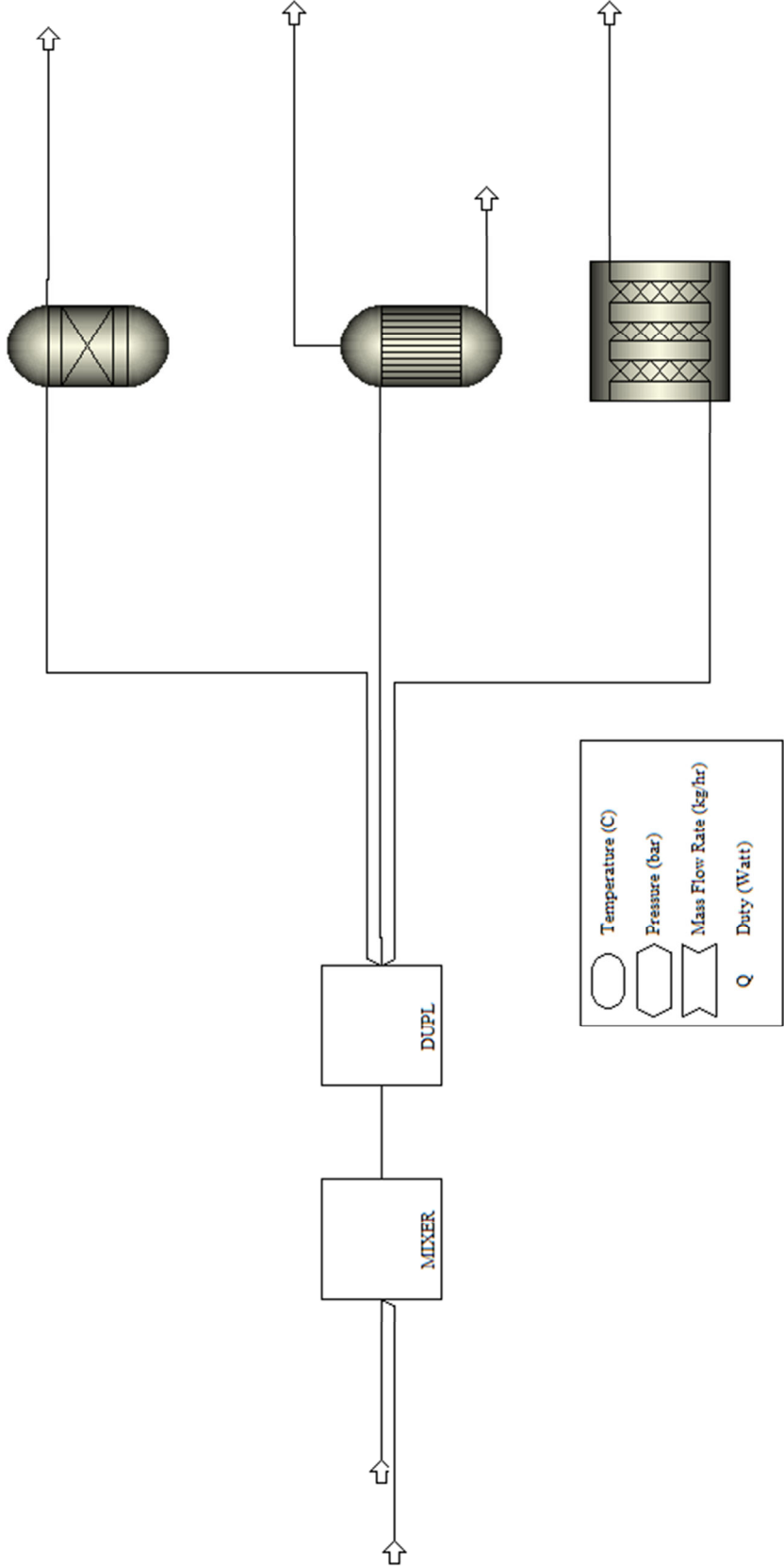




## Manganese

Note: Manganese data is not presented as it is not used for an Aspen plus model elaboration.

# Appendix VI – New Aspen Plus CLR flow-sheet with tested reactors



# Appendix VII – Molar balance values for ASPEN input data

750

| Components    |       | IN (l)  |         |         |     | OUT (l) |         |         |         |
|---------------|-------|---------|---------|---------|-----|---------|---------|---------|---------|
| H2            | 22,8  | 0,30528 | 0,01363 | 0,02726 | 2   |         |         |         |         |
| CO            | 33,0  | 0,44096 | 0,01969 | 0,55120 | 28  | 0,01969 | 0,01969 |         |         |
| CO2           | 15,3  | 0,20490 | 0,00915 | 0,40249 | 44  | 0,00915 | 0,01830 |         |         |
| CH4           | 12,4  | 0,16577 | 0,00740 | 0,11841 | 16  | 0,00740 | 0,02960 |         |         |
| C2H2          | 0,4   | 0,00485 | 0,00022 | 0,00563 | 26  | 0,00043 | 0,00043 |         |         |
| C2H4          | 4,3   | 0,05739 | 0,00256 | 0,07174 | 28  | 0,00512 | 0,01025 |         |         |
| C2H6          | 0,4   | 0,00525 | 0,00023 | 0,00703 | 30  | 0,00047 | 0,00141 |         |         |
| C3H8          | 0,2   | 0,00275 | 0,00012 | 0,00540 | 44  | 0,00037 | 0,00098 |         |         |
| N2            | 11,2  | 0,14930 | 0,00667 | 0,18663 | 28  |         |         | 0,01333 |         |
| O2            | 0,0   | 0,00000 | 0,00000 | 0,00000 | 32  |         | 0,00000 |         |         |
| Tars          |       | 0,00637 | 0,00028 | 0,03641 | 128 | 0,00284 | 0,00228 |         |         |
| H2O           |       | 1,50657 | 0,06726 | 1,21063 | 18  |         | 0,13451 | 0,06726 |         |
| Transp. O2 AR | 0,0   | 0,04216 | 0,00188 | 0,06023 | 32  |         | 0,00376 |         |         |
| Humid         | 100,0 | 2,89157 | 0,12909 | 2,68306 |     | 0,04547 | 0,20672 | 0,10900 | 0,01333 |
| Dry           |       | 1,38500 | 0,06183 | 1,47243 |     | 0,04547 | 0,07221 | 0,04175 | 0,01333 |
| Dry           | mol%  |         |         |         |     |         |         |         |         |
| Humid         | 100,0 | 2       | 0,08929 | 1,63725 |     | 0,04475 | 0,08669 | 0,04898 | 0,01333 |
|               |       | 3,33920 | 0,12746 | 2,70867 |     | 0,04475 | 0,20574 | 0,10850 | 0,01333 |
| H2            | 24,2  | 0,48364 | 0,02159 | 0,04318 | 2   |         | 0,04318 |         |         |
| CO            | 10,5  | 0,20950 | 0,00935 | 0,26188 | 28  | 0,00935 | 0,00935 |         |         |
| CO2           | 22,2  | 0,44382 | 0,01981 | 0,87179 | 44  | 0,01981 | 0,03963 |         |         |
| CH4           | 8,4   | 0,16868 | 0,00753 | 0,12049 | 16  | 0,00753 | 0,03012 |         |         |
| C2H2          | 0,0   | 0,00060 | 0,00003 | 0,00070 | 26  | 0,00005 | 0,00005 |         |         |
| C2H4          | 2,7   | 0,05483 | 0,00245 | 0,06853 | 28  | 0,00490 | 0,00979 |         |         |
| C2H6          | 0,3   | 0,00540 | 0,00024 | 0,00724 | 30  | 0,00048 | 0,00145 |         |         |
| C3H8          | 0,0   | 0,00000 | 0,00000 | 0,00000 | 44  | 0,00000 | 0,00000 |         |         |
| N2            | 7,5   | 0,14932 | 0,00667 | 0,18664 | 28  |         |         | 0,01333 |         |
| O2            | 0,0   | 0,00000 | 0,00000 | 0,00000 | 32  |         | 0,00000 |         |         |
| Tars          |       | 0,00587 | 0,00026 | 0,03356 | 128 | 0,00262 | 0,00210 |         |         |
| H2O           |       | 1,33332 | 0,05952 | 1,07142 | 18  |         | 0,11905 | 0,05952 |         |
| He            | 24,2  | 0,48420 | 0,02162 | 0,04323 | 2   |         |         |         |         |

Vm(L/mole) 22,4

|                             |                              |
|-----------------------------|------------------------------|
| Tars IN (g/m <sup>3</sup> ) | Tars OUT (g/m <sup>3</sup> ) |
| 27,24                       | 16,78                        |
| (g/l)                       | (g/l)                        |
| 0,02724                     | 0,01678                      |

|              |               |
|--------------|---------------|
| H2O IN (g/l) | H2O OUT (g/l) |
| 0,90585      | 0,53571       |

|                        |       |
|------------------------|-------|
| C increase % (total)   | -1,6  |
| C increase % (on tars) | -28,9 |

|                        |       |
|------------------------|-------|
| H increase % (total)   | -0,5  |
| H increase % (on tars) | -28,9 |

|             |             |
|-------------|-------------|
| He          | % in the FR |
| SLS [L/min] | 86,5        |
| 0,35        | 0,21        |

|                       |   |
|-----------------------|---|
| Dry gas FR out(l/min) | 2 |
|-----------------------|---|

|               |        |               |
|---------------|--------|---------------|
| AR            | In     | N2 IN (L/min) |
| O2 IN (L/min) | 5,2454 |               |
| 0,0546        |        |               |

|             |             |             |        |             |
|-------------|-------------|-------------|--------|-------------|
| Out (l)     | CO2         | O2          | He     | N2          |
| mol%        | 0,21        | 0,02        | -      | 5,320699484 |
| flow(l/min) | 0,011358774 | 0,001081788 | 0,0758 |             |

# 800

| Components    | IN (l)   |         |         |         |     |         |         |         |         |  | OUT (l) |  |  |  |  |  |  |  |         |  |
|---------------|----------|---------|---------|---------|-----|---------|---------|---------|---------|--|---------|--|--|--|--|--|--|--|---------|--|
|               |          |         |         |         |     |         |         |         |         |  |         |  |  |  |  |  |  |  |         |  |
| H2            | 22.8     | 0.27931 | 0.01247 | 0.02494 | 2   | 0.01801 | 0.02494 |         |         |  |         |  |  |  |  |  |  |  |         |  |
| CO            | 33.0     | 0.40344 | 0.01801 | 0.50430 | 28  | 0.00837 | 0.01801 |         |         |  |         |  |  |  |  |  |  |  |         |  |
| CO2           | 15.3     | 0.18747 | 0.00837 | 0.36825 | 44  | 0.00837 | 0.01674 |         |         |  |         |  |  |  |  |  |  |  |         |  |
| CH4           | 12.4     | 0.15167 | 0.00677 | 0.10833 | 16  | 0.00677 | 0.02708 |         |         |  |         |  |  |  |  |  |  |  |         |  |
| C2H2          | 0.4      | 0.00444 | 0.00020 | 0.00515 | 26  | 0.00040 | 0.00040 |         |         |  |         |  |  |  |  |  |  |  |         |  |
| C2H4          | 4.3      | 0.05251 | 0.00234 | 0.06563 | 28  | 0.00469 | 0.00938 |         |         |  |         |  |  |  |  |  |  |  |         |  |
| C2H6          | 0.4      | 0.00481 | 0.00021 | 0.00644 | 30  | 0.00043 | 0.00129 |         |         |  |         |  |  |  |  |  |  |  |         |  |
| C3H8          | 0.2      | 0.00252 | 0.00011 | 0.00494 | 44  | 0.00034 | 0.00090 |         |         |  |         |  |  |  |  |  |  |  |         |  |
| N2            | 11.2     | 0.13660 | 0.00610 | 0.17075 | 28  |         |         |         |         |  |         |  |  |  |  |  |  |  | 0.01220 |  |
| O2            | 0.0      | 0.00000 | 0.00000 | 0.00000 | 32  |         |         |         |         |  |         |  |  |  |  |  |  |  |         |  |
| Tars          | ?        | 0.00583 | 0.00026 | 0.03331 | 128 | 0.00260 | 0.00208 |         |         |  |         |  |  |  |  |  |  |  |         |  |
| H2O           |          | 1.37838 | 0.06153 | 1.10763 | 18  | 0.12307 | 0.06153 |         |         |  |         |  |  |  |  |  |  |  |         |  |
| Transp. O2 AR |          | 0.04182 | 0.00187 | 0.05975 | 32  | 0.00373 | 0.00373 |         |         |  |         |  |  |  |  |  |  |  |         |  |
| Humid         | 100      | 2.64878 | 0.11825 | 2.45942 |     | 0.04160 | 0.18913 | 0.10002 | 0.01220 |  |         |  |  |  |  |  |  |  |         |  |
| Dry           |          | 1.27041 | 0.05671 | 1.35179 |     | 0.04160 | 0.06606 | 0.03848 | 0.01220 |  |         |  |  |  |  |  |  |  |         |  |
| Dry           | DRY mol% |         |         |         |     |         |         |         |         |  |         |  |  |  |  |  |  |  |         |  |
| Humid         | 100      | 2       | 0.08929 | 1.60030 |     | 0.04089 | 0.08586 | 0.04838 | 0.01493 |  |         |  |  |  |  |  |  |  |         |  |
|               |          | 3.15066 | 0.12025 | 2.52164 |     | 0.04089 | 0.18823 | 0.09956 | 0.01493 |  |         |  |  |  |  |  |  |  |         |  |
| H2            | 27.1     | 0.54211 | 0.02420 | 0.04840 | 2   | 0.00811 | 0.04840 |         |         |  |         |  |  |  |  |  |  |  |         |  |
| CO            | 9.1      | 0.18164 | 0.00811 | 0.22705 | 28  | 0.00811 | 0.00811 |         |         |  |         |  |  |  |  |  |  |  |         |  |
| CO2           | 22.5     | 0.45099 | 0.02013 | 0.88588 | 44  | 0.02013 | 0.04027 |         |         |  |         |  |  |  |  |  |  |  |         |  |
| CH4           | 8.0      | 0.16001 | 0.00714 | 0.11429 | 16  | 0.00714 | 0.02857 |         |         |  |         |  |  |  |  |  |  |  |         |  |
| C2H2          | 0.0      | 0.00060 | 0.00003 | 0.00070 | 26  | 0.00005 | 0.00005 |         |         |  |         |  |  |  |  |  |  |  |         |  |
| C2H4          | 1.9      | 0.03885 | 0.00173 | 0.04856 | 28  | 0.00347 | 0.00694 |         |         |  |         |  |  |  |  |  |  |  |         |  |
| C2H6          | 0.1      | 0.00160 | 0.00007 | 0.00215 | 30  | 0.00014 | 0.00043 |         |         |  |         |  |  |  |  |  |  |  |         |  |
| C3H8          | 0.0      | 0.00000 | 0.00000 | 0.00000 | 44  | 0.00000 | 0.00000 |         |         |  |         |  |  |  |  |  |  |  |         |  |
| N2            | 8.4      | 0.16719 | 0.00746 | 0.20899 | 28  |         |         |         |         |  |         |  |  |  |  |  |  |  | 0.01493 |  |
| O2            | 0.0      | 0.00000 | 0.00000 | 0.00000 | 32  |         |         |         |         |  |         |  |  |  |  |  |  |  |         |  |
| Tars          |          | 0.00411 | 0.00018 | 0.02348 | 128 | 0.00183 | 0.00147 |         |         |  |         |  |  |  |  |  |  |  |         |  |
| H2O           |          | 1.14655 | 0.05119 | 0.92134 | 18  | 0.10237 | 0.05119 |         |         |  |         |  |  |  |  |  |  |  |         |  |
| He            | 22.9     | 0.45700 | 0.02040 | 0.04080 | 2   |         |         |         |         |  |         |  |  |  |  |  |  |  |         |  |

Vnl(L/mole) 22.4

Tars IN (g/m3) 27.24 Tars OUT (g/m3) 11.74

(g/l) 0.02724 (g/l) 0.01174

H2O IN (g/l) 0.90585 H2O OUT (g/l) 0.46067

C Increase % (total) -1.7

C Increase % (on tars) -48.7

H Increase % (total) -0.5

H Increase % (on tars) -48.7

He He % in the FR 81.6

SLS [L/min] 0.35 ILS [L/min] 0.21

Dry gas FR out(L/min) 2

AR In AR Out (l) 5.2454

O2 IN (L/min) 0.0546 N2 IN (L/min) 5.2454

mol% flow(L/min) CO2(0.21) 0.21 O2(0.02) 0.02 He - N2 5.43997284